Nonlinear Dynamics (2005) 40: 251–279

Global Bifurcations and Chaotic Dynamics in Nonlinear Nonplanar Oscillations of a Parametrically Excited Cantilever Beam

WEI ZHANG[1,*], FENGXIA WANG[2], and MINGHUI YAO[1]

[1]*College of Mechanical Engineering, Beijing University of Technology, Beijing 100022, P.R. China;* [2]*School of Mechanical Engineering, Purdue University, West Lafayette, IN 47907, U.S.A.; *Author for correspondence (e-mail: sandyzhang0@yahoo.com; fax: +86-10-67391617)*

(Received: 13 February 2004; accepted: 3 November 2004)

Abstract. This paper presents the analysis of the global bifurcations and chaotic dynamics for the nonlinear nonplanar oscillations of a cantilever beam subjected to a harmonic axial excitation and transverse excitations at the free end. The governing nonlinear equations of nonplanar motion with parametric and external excitations are obtained. The Galerkin procedure is applied to the partial differential governing equation to obtain a two-degree-of-freedom nonlinear system with parametric and forcing excitations. The resonant case considered here is 2:1 internal resonance, principal parametric resonance-1/2 subharmonic resonance for the in-plane mode and fundamental parametric resonance–primary resonance for the out-of-plane mode. The parametrically and externally excited system is transformed to the averaged equations by using the method of multiple scales. From the averaged equation obtained here, the theory of normal form is applied to find the explicit formulas of normal forms associated with a double zero and a pair of pure imaginary eigenvalues. Based on the normal form obtained above, a global perturbation method is utilized to analyze the global bifurcations and chaotic dynamics in the nonlinear nonplanar oscillations of the cantilever beam. The global bifurcation analysis indicates that there exist the heteroclinic bifurcations and the Silnikov type single-pulse homoclinic orbit in the averaged equation for the nonlinear nonplanar oscillations of the cantilever beam. These results show that the chaotic motions can occur in the nonlinear nonplanar oscillations of the cantilever beam. Numerical simulations verify the analytical predictions.

Key words: cantilever beam, chaotic dynamics, global bifurcations, nonlinear nonplanar oscillations, normal form, parametric and external excitations

1. Introduction

It is well known that the nonlinear nonplanar dynamics of the cantilever beams are the subjects of interest because of their importance in many applications to spacecraft station, satellite antenna and flexible manipulator. Therefore, research on the nonlinear nonplanar dynamics of the cantilever beams has received considerable attention. As the development of the theory of nonlinear dynamics, predictions and understanding become possible for more complicated nonlinear phenomena in flexible cantilever beams, such as the global bifurcations and Silnikov type chaotic dynamics.

Since the work given by Crespo da Silva and Glynn [1], the nonlinear nonplanar dynamics and response of flexible cantilever beams have been investigated by several researchers. Crespo da Silva and Glynn [1, 2] formulated a set of integral–partial differential governing equations of motion describing the nonlinear nonplanar oscillations of an inextensional cantilever beam and utilized the method of multiple scales to analyze forced resonant oscillations of the cantilever beam. Crespo da Silva and Glynn [3] investigated the nonlinear nonplanar, flexural–torsional oscillations of a clamped–clamped/sliding beam under a planar distributed harmonic excitation. In another paper [4], the nonlinear nonplanar oscillations and response of a cantilever beam with asymmetric support conditions were studied by Crespo da Silva and Glynn. Zaretzky and Crespo da Silva [5] gave an experimental investigation for the nonlinear nonplanar motion of the cantilever beams excited by a periodic transverse base vibration.

Besides the above researches on the nonlinear nonplanar dynamics and response of flexible cantilever beams given by Crespo da Silva et al., there are also other researches worth mentioning. Nayfeh and Pai [6] used the Galerkin procedure and the method of multiple scales to investigate the nonlinear planar and nonplanar responses of the inextensional cantilever beams and found that the nonlinear geometric terms produce a hardening effect and dominate the nonplanar responses for all modes. The nonplanar responses of a cantilevered beam subject to lateral harmonic base-excitation were also analyzed by Pai and Nayfeh [7] using two nonlinear coupled integro-differential equations of motion. Cusumano and Moon [8, 9] presented results for an externally excited thin elastica. Anderson et al. [10] analytically and experimentally investigated the response of the cantilever beam with widely separated natural frequencies and observed that the responses consist of the first, third, and fourth modes. Arafat et al. [11] studied the nonlinear nonplanar response of cantilever inextensional metallic beams to a principal parametric excitation and found that there exist the bifurcations and chaotic motion. Esmailzadeh and Nakhaie-Jazar [12] investigated the nonlinear parametric vibration of a massless cantilever beam with a lumped mass attached to its free end while being excited harmonically at the base. Hamdan et al. [13] analyzed the second order approximations of the nonlinear planar responses and the steady-state principal parametric resonance response of a vertically mounted flexible cantilever beam subjected to a vertical harmonic base motion. Siddiqui et al. [14] analyzed large amplitude motion of a cantilever beam carrying a moving spring-mass and obtained the nonlinear responses. Malatkar and Nayfeh [15] gave experimental and theoretical study of the nonlinear response of a flexible cantilever beam to an external harmonic excitation. Their results demonstrated the energy transfer from the third mode to the first mode. Young and Juan [16] studied the nonlinear response of a fluttered, cantilevered beam subjected to a random follower force at the free end.

The global bifurcations and chaotic dynamics of high-dimensional nonlinear systems have been at the forefront of nonlinear dynamics for the last two decades. The global bifurcations and chaotic dynamics for high-dimensional nonlinear systems are an important theoretical problem in science and engineering applications as they can reveal the instabilities of motion and complicated dynamical behaviors in high-dimensional nonlinear systems. However, due to lack of analytical tools to study global bifurcations and chaotic dynamics for high-dimensional nonlinear systems, it is extremely challenging to develop the theories of global bifurcations and chaotic dynamics for high-dimensional nonlinear systems and to give systematic applications to engineering problems. Despite the challenge, certain progress has been achieved in this field in the past two decades.

Wiggins [17] divided four-dimensional perturbed Hamiltonian systems into three types and utilized the Melnikov method to investigate the global bifurcations and chaotic dynamics for these three basic systems. Based on study given by Wiggins [17], Kovacic and Wiggins [18] developed a new global perturbation techniques which may be used to detect the Silnikov type single-pulse homoclinic and heteroclinic orbits in four-dimensional autonomous ordinary differential equations. Using this method, they gave an application to the forced and damped sine-Gordon equation. Later on, Kovacic and Wettergren [19] employed a modified Melnikov method to study the existence of multi-pulse jumping of homoclinic orbits and chaotic dynamics in resonantly forced coupled pendula. Furthermore, Kaper and Kovacic [20] investigated the existence of several types of multi-bump homoclinic orbits to resonance bands for completely integral Hamiltonian systems subjected to small amplitude Hamiltonian and damped perturbations. Camassa et al. [21] extended the Melnikov method to investigate multi-pulse jumping of homoclinic and heteroclinic orbits in a class of perturbed Hamiltonian systems. In the meantime, the energy-phase method was first presented by Haller and Wiggins [22] where single-pulse homoclinic orbits to a resonance in the Hamiltonian case were studied. Subsequently, Haller and Wiggins [23, 24] further developed the energy-phase method and used it to study the existence of multi-pulse jumping

of homoclinic orbits in the damped-forced nonlinear Schrodinger equation and perturbed Hamiltonian systems. Recently, Haller [25] summarized the energy-phase method and presented a detailed procedure of application to the problems in mechanics and engineering.

Besides the aforementioned researches on the theories of global bifurcations and chaotic dynamics in high-dimensional nonlinear systems, it is worth mentioning researches on applying the developed theories to engineering applications. Feng and Wiggins [26] employed the global perturbation techniques to investigate the global bifurcations and chaotic dynamics for parametrically excited mechanical systems with O(2) and $Z_2 \oplus Z_2$ symmetries. Feng and Sethna [27] made use of a global perturbation method to study the global bifurcations and chaotic dynamics of thin plate under parametric excitation and obtained the conditions in which the Silnikov type homoclinic orbits and chaos can occur. Feng and Liew [28] analyzed the existence of the Silnikov homoclinic orbits in the averaged equations which represent the modal interactions between two modes with zero-to-one internal resonance and influence of the fast mode on the slow mode. The global dynamics of parametrically excited nonlinear reversible systems with non-semisimple 1:1 resonance was also considered by Malhotra and Sri Namachchivaya [29]. Malhotra and Sri Namachchivaya [30] used the averaging method and the Melnikov technique to study local, global bifurcations and chaos of a two-degree-of-freedom shallow arch subjected to simple harmonic excitation for case of internal resonance. Recently, Malhotra et al. [31] used the energy-phase method to investigate multi-pulse homoclinic orbits and chaotic dynamics in the motion of flexible spinning discs. The extended subharmonic Melnikov method and the modified homoclinic Melnikov method were employed by Yagasaki [32] to analyze periodic orbits and homoclinic motions in periodically forced, weakly coupled oscillators with the perturbations. The global bifurcations and chaotic dynamics were investigated by Zhang et al. [33] and Zhang [34] for both parametrically externally excited and parametrically excited simply supported rectangular thin plates. Furthermore, Zhang and Li [35] employed the global perturbation approach to investigate the global bifurcations and chaotic dynamics for a two-degree-of-freedom nonlinear vibration absorber. Recently, Zhang and Tang [36] studied the global bifurcations and chaotic dynamics of the suspended elastic cable to small tangential vibration of one support which causes simultaneously the parametric excitation of out-of-plane motion and the parametric and external excitations of in-plane motion.

This paper aims at studying the global bifurcations and chaotic dynamics for the nonlinear nonplanar oscillations of a cantilever beam subjected to a harmonic axial excitation and transverse excitations at the free end. The work is focused on the case of 2:1 internal resonance, principal parametric resonance-1/2 subharmonic resonance for the in-plane mode and fundamental parametric resonance–primary resonance for the out-of-plane mode. First, the governing nonlinear equation of nonplanar motion with parametric excitation is obtained. The Galerkin procedure is applied to the partial governing equation to obtain a two-degree-of-freedom nonlinear system under combined parametric and forcing excitations. Then, using the method of multiple scales, the parametrically and externally excited two-degree-of-freedom nonlinear system is transformed to the averaged equations. From the averaged equation, the theory of normal form is applied to find the explicit formulas of normal form associated with a double zero and a pair of pure imaginary eigenvalues. Finally, a global perturbation method presented by Kovacic and Wiggins [18] is employed to analyze the global bifurcations and chaotic dynamics for the nonlinear nonplanar oscillations of the cantilever beam subjected to a harmonic axial excitation and transverse excitations at the free end. The global bifurcation analysis indicates that there exist the heteroclinic bifurcations and the Silnikov type single-pulse homoclinic orbit in the averaged equation. The results obtained by using numerical simulation also show that the chaotic motion can occur in the nonlinear nonplanar oscillations of the cantilever beam subjected to a harmonic axial excitation and transverse excitations at the free end, which verifies the analytical prediction.

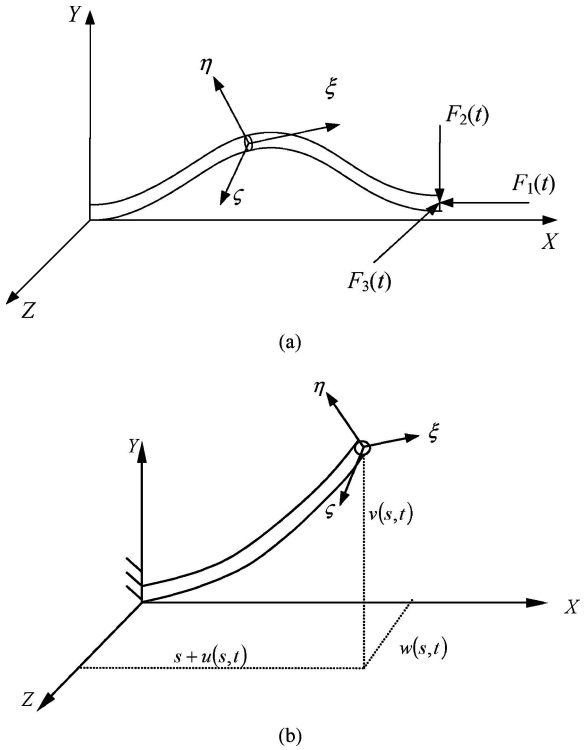

Figure 1. The model of a cantilever beam with length L, mass m per unit length and subjected to a harmonic axial excitation and transverse excitations at the free end, (a) the model; (b) a segment.

2. Equations of Motion and Perturbation Analysis

We consider a cantilever beam with length L, mass m per unit length and subjected to a harmonic axial excitation and transverse excitations at the free end, as shown in Figure 1(a). Assume that the beam considered here is the Euler–Bernoulli beam. A Cartesian coordinate system, $Oxyz$, is adopted which is located in the symmetric plane of the cantilever beam. The s denotes the curve coordinate along the elastic axis before deformation. The ξ, η and ζ are the principal axes of the cross section for the cantilever beam at position s. The symbols $v(s,\ t)$ and $w(s,\ t)$ denote the displacements of a point in the middle line of the cantilever beam in the y and z directions, respectively, as shown in Figure 1(b). The harmonic axial excitation may be expressed in the form $2F_1 \cos \Omega_1 t$. The transverse excitations in the y and z directions are represented in the forms $2F_2(s) \cos \Omega_2 t$ and $2F_3(s) \cos \Omega_2 t$, respectively. The non-dimensional governing equations of the nonlinear nonplanar motion for the cantilever beam under combined parametric and forcing excitations are of the following form [37]

$$\ddot{v} + \bar{c}\dot{v} + \beta_y v^{iv} + F_1 \cos(\Omega_1 t) v'' = (1-\beta_y)\left[w'' \int_1^s v''w''ds - w''' \int_0^s v''w'ds\right]'$$
$$- \frac{1}{\beta_\gamma}(1-\beta_y)^2\left[w'' \int_0^s \int_1^s v''w''dsds\right]'' - \beta_y[v'(v'v'' + w'w'')']'$$
$$- \frac{1}{2}\left[v' \int_1^s \frac{d^2}{dt^2}\left\{\int_0^s (v'^2 + w'^2)ds\right\}ds\right]' - F_1 \cos(\Omega_1 t)[v'(v'^2 + w'^2)]' + F_2(s)\cos(\Omega_2 t), \qquad (1a)$$

$$\ddot{w} + \bar{c}\dot{w} + w^{iv} + F_1 \cos(\Omega_1 t) w'' = -(1-\beta_y)\left[v'' \int_1^s v'' w'' ds - v''' \int_0^s w'' v' ds\right]'$$
$$- \frac{1}{\beta_\gamma}\left(1-\beta_y\right)^2 \left[v'' \int_0^s \int_1^s v'' w'' ds ds\right]'' - [w'(v'v'' + w'w'')']'$$
$$- \frac{1}{2}\left[w' \int_1^s \frac{d^2}{dt^2}\left\{\int_0^s (v'^2 + w'^2) ds\right\} ds\right]' - F_1 \cos(\Omega_1 t)[w'(v'^2 + w'^2)]' + F_3(s)\cos(\Omega_2 t), \quad (1b)$$

where the dots and primes, respectively, represent partial differentiation with respect to t and x, $\bar{c}$ is the damping coefficient, and β_y is the ratio between the in-plane and out-of-plane principal flexural stiffnesses, that is, $\beta_y = D_\varsigma / D_\eta$.

The boundary conditions are

$$v(0,\ t) = w(0,\ t) = v'(0,\ t) = w'(0,\ t) = 0, \quad (2a)$$
$$v''(1,\ t) = w''(1,\ t) = v'''(1,\ t) = w'''(1,\ t) = 0. \quad (2b)$$

In the following analysis, we apply the Galerkin procedure to Equation (1) to obtain a two-degree-of-freedom nonlinear system under combined parametric and forcing excitations. The planar and nonplanar flexural modes for the cantilever beam are considered as

$$v(s,\ t) = y(t)G(s), \quad (3a)$$
$$w(s,\ t) = z(t)G(s), \quad (3b)$$

where the function $G(s)$ is a linear mode of transverse free vibration for the cantilever beam and is of the following form

$$G(s) = \cosh(rs) - \cos(rs) - [(\cosh(r) + \cos(r))/(\sinh(r) + \sin(r))][\sinh(rs) - \sin(rs)]. \quad (4)$$

The linear mode $G(s)$ satisfies ordinary differential equation

$$G'''' - r^4 G = 0, \quad (5)$$

and

$$G(0) = G'(0) = G''(1) = G'''(1) = 0. \quad (6)$$

The r in Equation (5) is determined by the characteristic equation

$$\cosh(r)\cos(r) + 1 = 0. \quad (7)$$

Introduce the time variable $\hat{t} = r^2 t$. For convenience of the following analysis, we drop the hat. Substituting Equation (3) into Equation (1), multiplying Equation (1) by $G(s)$ and integrating to s from

0 to 1, a two-degree-of-freedom nonlinear system under combined parametric and forcing excitations is obtained as

$$\ddot{y} + c\dot{y} + \beta_y y - 2\alpha_1 F_1 \cos(\Omega_1 t) y + \alpha_2 y(y\ddot{y} + \dot{y}^2 + z\ddot{z} + \dot{z}^2) + \alpha_3 \beta_y y^3 + \left[\beta_y \alpha_3 + (1-\beta_y)\alpha_4 - \frac{1}{\beta_y}(1-\beta_y)^2 \alpha_5\right] y z^2 - 2\bar{F}_1 \cos(\Omega_1 t)(y^3 + y z^2) = f_1 \cos \Omega_2 t, \tag{8a}$$

$$\ddot{z} + c\dot{z} + z - 2\alpha_1 F_1 \cos(\Omega_1 t) z + \alpha_2 z(y\ddot{y} + \dot{y}^2 + z\ddot{z} + \dot{z}^2) + \alpha_3 z^3 - \left[(1-\beta_y)\alpha_4 + \frac{1}{\beta_y}(1-\beta_y)^2 \alpha_5 - \beta_y \alpha_3\right] z y^2 - 2\bar{F}_1 \cos(\Omega_1 t)(z^3 + z y^2) = f_2 \cos \Omega_2 t, \tag{8b}$$

where the dots denote partial differentiation with respect to $\hat{t}$, and

$$c = \frac{\bar{c}}{r^2}, \quad \alpha_1 = -\frac{1}{r^4}\int_0^1 G G'' ds, \quad \alpha_2 = \int_0^1 G\left[G' \int_1^s \int_0^s G'^2 ds ds\right]' ds,$$
$$\alpha_3 = \frac{1}{r^4}\int_0^1 G[G'(G'G'')']' ds, \quad \alpha_4 = -\frac{1}{r^4}\int_0^1 G\left[G'' \int_1^s G'^2 ds - G''' \int_0^s G' G'' ds\right]' ds,$$
$$\alpha_5 = -\frac{1}{r^4}\int_0^1 G\left[G'' \int_0^s \int_1^s G''^2 ds ds\right]'' ds, \quad \bar{F}_1 = -\frac{F_1}{2r^4}\int_0^1 G(G'^3)' ds,$$
$$f_1 = \frac{1}{r^4}\int_0^1 G F_2 ds, \quad f_2 = \frac{1}{r^4}\int_0^1 G F_3 ds. \tag{9}$$

To obtain a system which is suitable for the application of the method of multiple scales [38], the scale transformations may be introduced as

$$\alpha_2 \to \varepsilon\alpha_2, \quad \alpha_3 \to \varepsilon\alpha_3, \quad \alpha_4 \to \varepsilon\alpha_4, \quad \alpha_5 \to \varepsilon\alpha_5,$$
$$F_1 \to \varepsilon F_1, \quad \bar{F}_1 \to \varepsilon^2 \bar{F}_1, \quad c \to \varepsilon c, \quad f_1 \to \varepsilon f_1, \quad f_2 \to \varepsilon f_2, \tag{10}$$

where ε is a small perturbation parameter.

Substituting Equation (10) into Equation (8), we obtain the following dimensionless two-degree-of-freedom nonlinear system under combined parametric and forcing excitations

$$\ddot{y} + \varepsilon c\dot{y} + \beta_y y - 2\varepsilon\alpha_1 F_1 \cos(\Omega_1 t) y + \varepsilon\alpha_2 y(y\ddot{y} + \dot{y}^2 + z\ddot{z} + \dot{z}^2) + \varepsilon\alpha_3 \beta_y y^3 + \varepsilon\left[\beta_y \alpha_3 + (1-\beta_y)\alpha_4 - \frac{1}{\beta_y}(1-\beta_y)^2 \alpha_5\right] y z^2 - 2\varepsilon^2 \bar{F}_1 \cos(\Omega_1 t)(y^3 + y z^2) = \varepsilon f_1 \cos \Omega_2 t, \tag{11a}$$

$$\ddot{z} + \varepsilon c\dot{z} + z - 2\varepsilon\alpha_1 F_1 \cos(\Omega_1 t) z + \varepsilon\alpha_2 z(y\ddot{y} + \dot{y}^2 + z\ddot{z} + \dot{z}^2) + \varepsilon\alpha_3 z^3 + \varepsilon\left[\beta_y \alpha_3 - (1-\beta_y)\alpha_4 - \frac{1}{\beta_y}(1-\beta_y)^2 \alpha_5\right] z y^2 - 2\varepsilon^2 \bar{F}_1 \cos(\Omega_1 t)(z^3 + z y^2) = \varepsilon f_2 \cos \Omega_2 t, \tag{11b}$$

The above equations, which include the parametric and forcing excitations, describe the planar and nonplanar flexural nonlinear oscillation of the cantilever beam. In the following analysis, we will use the method of multiple scales to obtain the averaged equations.

We use the method of multiple scales [38] to find the uniform solutions of Equations (11) in the following form

$$y(t, \varepsilon) = y_0(T_0, T_1) + \varepsilon y_1(T_0, T_1) + \cdots, \tag{12a}$$

$$z(t, \varepsilon) = z_0(T_0, T_1) + \varepsilon z_1(T_0, T_1) + \cdots, \tag{12b}$$

where $T_0 = t, T_1 = \varepsilon t$.

Then, we have the differential operators

$$\frac{d}{dt} = \frac{\partial}{\partial T_0}\frac{\partial T_0}{\partial t} + \frac{\partial}{\partial T_1}\frac{\partial T_1}{\partial t} + \cdots = D_0 + \varepsilon D_1 + \cdots, \tag{13}$$

$$\frac{d^2}{dt^2} = (D_0 + \varepsilon D_1 + \cdots)^2 = D_0^2 + 2\varepsilon D_0 D_1 + \cdots, \tag{14}$$

where $D_k = \frac{\partial}{\partial T_k}$, $k = 0,\ 1$.

We investigate the case of the ratio $\beta_y = \omega_1^2 \approx 1/4$. In this case, there is the relation of 2:1 internal resonance for Equation (11). In addition, principal parametric resonance-1/2 subharmonic resonance for the in-plane mode and fundamental parametric resonance–primary resonance for the out-of-plane mode are considered. The resonant relations are represented as

$$\Omega_1 = \Omega_2, \quad \omega_1^2 = \beta_y = \frac{1}{4}\Omega_1^2 + \varepsilon\sigma_1, \quad 1 = \omega_2^2 = \Omega_1^2 + \varepsilon\sigma_2, \tag{15}$$

where σ_1 and σ_2 are two detuning parameters. For convenience of the following analysis, let $\Omega_1 = 1$.

Substituting Equations (12)–(15) into Equation (11) and balancing the coefficients of like power of ε yield the following differential equations

order ε^0

$$D_0^2 y_0 + \frac{1}{4} y_0 = 0, \tag{16a}$$

$$D_0^2 z_0 + z_0 = 0, \tag{16b}$$

order ε^1

$$\begin{aligned} D_0^2 y_1 + \frac{1}{4} y_1 = {} & -2D_0 D_1 y_0 - cD_0 y_0 - \sigma_1 y_0 + \alpha_1 F_1\left(e^{iT_0} + e^{-iT_0}\right) y_0 \\ & - \alpha_2 y_0\left[y_0 D_0^2 y_0 + (D_0 y_0)^2 + z_0 D_0^2 z_0 + (D_0 z_0)^2\right] - \frac{1}{4}\alpha_3 y_0^3 \\ & - \left(\frac{1}{4}\alpha_3 + \frac{3}{4}\alpha_4 - \frac{9}{4}\alpha_5\right) y_0 z_0^2 + \frac{1}{2} f_1\left(e^{iT_0} + e^{-iT_0}\right), \end{aligned} \tag{17a}$$

$$\begin{aligned} D_0^2 z_1 + z_1 = {} & -2D_0 D_1 z_0 - cD_0 z_0 - \sigma_2 z_0 + \alpha_1 F_1\left(e^{iT_0} + e^{-iT_0}\right) z_0 \\ & - \alpha_2 z_0\left[y_0 D_0^2 y_0 + (D_0 y_0)^2 + z_0 D_0^2 z_0 + (D_0 z_0)^2\right] - \alpha_3 z_0^3 \\ & - \left(\alpha_3 - \frac{3}{4}\alpha_4 - \frac{9}{4}\alpha_5\right) z_0 y_0^2 + \frac{1}{2} f_2\left(e^{iT_0} + e^{-iT_0}\right). \end{aligned} \tag{17b}$$

The solutions of Equations (16) in the complex form can be expressed as

$$y_0 = A(T_1)e^{i\frac{1}{2}T_0} + \bar{A}(T_1)e^{-i\frac{1}{2}T_0}, \tag{18a}$$

$$z_0 = B(T_1)e^{iT_0} + B(T_1)e^{-iT_0}, \tag{18b}$$

where $\bar{A}$ and $\bar{B}$ are the parts of the complex conjugate of A and B.

Substituting Equations (18) into Equation (17) yields

$$\begin{aligned} D_0^2 y_1 + \frac{1}{4} y_1 = {} & \left[-iD_1 A - i\frac{1}{2}cA - \sigma_1 A + \alpha_1 F_1 \bar{A} + \frac{1}{2}\left(\alpha_2 - \frac{3}{2}\alpha_3\right) A^2 \bar{A}\right. \\ & \left. - \frac{1}{2}\left(\alpha_3 + 3\alpha_4 - 9\alpha_5\right) AB\bar{B}\right] e^{i\frac{1}{2}T_0} + \text{cc} + \text{NST}, \end{aligned} \tag{19a}$$

$$D_0^2 z_1 + z_1 = \left[-2iD_1B - icB - \sigma_2 B + (2\alpha_2 - 3\alpha_3) B^2\bar{B} - 2\left(\alpha_3 - \frac{3}{4}\alpha_4 - \frac{9}{4}\alpha_5\right) BA\bar{A} + \frac{1}{2} f_2\right] e^{iT_0} + \text{cc} + \text{NST}, \tag{19b}$$

where symbol cc and NST, respectively, denote the parts of the complex conjugate of the functions on the right-hand side of Equations (19) and the non-secular terms.

Eliminating the terms that produce secular terms from Equations (19), we obtain the averaged equations in the complex form

$$D_1 A = -\frac{1}{2}cA + i\sigma_1 A - i\alpha_1 F_1 \bar{A} - i\frac{1}{2}\left(\alpha_2 - \frac{3}{2}\alpha_3\right) A^2\bar{A} + i\frac{1}{2}(\alpha_3 + 3\alpha_4 - 9\alpha_5) AB\bar{B}, \tag{20a}$$

$$D_1 B = -\frac{1}{2}cB + i\frac{1}{2}\sigma_2 B - i\left(\alpha_2 - \frac{3}{2}\alpha_3\right) B^2\bar{B} + i\left(\alpha_3 - \frac{3}{4}\alpha_4 - \frac{9}{4}\alpha_5\right) BA\bar{A} - i\frac{1}{4} f_2. \tag{20b}$$

The functions A and B may be denoted in the Cartesian form

$$A(T_1) = \frac{1}{2}\left[x_1(T_1) + ix_2(T_1)\right], \tag{21a}$$

$$B(T_1) = \frac{1}{2}\left[x_3(T_1) + ix_4(T_1)\right], \tag{21b}$$

where the variables x_n ($n = 1, 2, 3, 4$) are the real functions with respect to T_1. Substituting Equations (21) into Equation (20), separating the real and imaginary parts, and solving for $\frac{dx_n}{dT_1}$ ($n = 1, 2, 3, 4$) from the resulting equations, the averaged equations in the Cartesian form are obtained as follows

$$\dot{x}_1 = -\frac{1}{2}cx_1 - (\sigma_1 + \alpha_1 F_1) x_2 + \frac{1}{16}(2\alpha_2 - 3\alpha_3) x_2\left(x_1^2 + x_2^2\right) - \beta_1 x_2\left(x_3^2 + x_4^2\right), \tag{22a}$$

$$\dot{x}_2 = (\sigma_1 - \alpha_1 F_1) x_1 - \frac{1}{2}cx_2 - \frac{1}{16}(2\alpha_2 - 3\alpha_3) x_1\left(x_1^2 + x_2^2\right) + \beta_1 x_1\left(x_3^2 + x_4^2\right), \tag{22b}$$

$$\dot{x}_3 = -\frac{1}{2}cx_3 - \frac{1}{2}\sigma_2 x_4 + \frac{1}{8}(2\alpha_2 - 3\alpha_3) x_4\left(x_3^2 + x_4^2\right) - \beta_2 x_4\left(x_1^2 + x_2^2\right), \tag{22c}$$

$$\dot{x}_4 = -\frac{1}{2}f_2 + \frac{1}{2}\sigma_2 x_3 - \frac{1}{2}cx_4 - \frac{1}{8}(2\alpha_2 - 3\alpha_3) x_3\left(x_3^2 + x_4^2\right) + \beta_2 x_3\left(x_1^2 + x_2^2\right), \tag{22d}$$

where $\beta_1 = \frac{1}{8}(\alpha_3 + 3\alpha_4 - 9\alpha_5)$, $\beta_2 = \frac{1}{16}(4\alpha_3 - 3\alpha_4 - 9\alpha_5)$.

In the next section, we will use the Maple program given by Zhang et al. [39] to obtain normal form of averaged Equations (22) for the nonlinear nonplanar oscillations of the cantilever beam under combined parametric and forcing excitations.

3. Computation of Normal Form

In order to conveniently analyze the global bifurcations and chaotic dynamics for the nonlinear nonplanar oscillations of the cantilever beam subjected to a harmonic axial excitation and transverse excitations at the free end, we need to reduce averaged Equations (22) to a simpler normal form. It is seen that there are $Z_2 \oplus Z_2$ and D_4 symmetries in averaged Equations (22) without the parameters. Therefore, these symmetries are also held in normal form.

Take into account the exciting amplitude f_2 as a perturbation parameter. Amplitude f_2 can be considered as an unfolding parameter when the global bifurcations are investigated. Obviously, when we do not consider the perturbation parameter, Equations (22) becomes

$$\dot{x}_1 = -\frac{1}{2}cx_1 - (\sigma_1 + \alpha_1 F_1)x_2 + \frac{1}{16}(2\alpha_2 - 3\alpha_3)\,x_2\left(x_1^2 + x_2^2\right) - \beta_1 x_2\left(x_3^2 + x_4^2\right), \tag{23a}$$

$$\dot{x}_2 = (\sigma_1 - \alpha_1 F_1)x_1 - \frac{1}{2}cx_2 - \frac{1}{16}(2\alpha_2 - 3\alpha_3)\,x_1\left(x_1^2 + x_2^2\right) + \beta_1 x_1\left(x_3^2 + x_4^2\right), \tag{23b}$$

$$\dot{x}_3 = -\frac{1}{2}cx_3 - \frac{1}{2}\sigma_2 x_4 + \frac{1}{8}(2\alpha_2 - 3\alpha_3)\,x_4\left(x_4^2 + x_3^2\right) - \beta_2 x_4\left(x_1^2 + x_2^2\right), \tag{23c}$$

$$\dot{x}_4 = \frac{1}{2}\sigma_2 x_3 - \frac{1}{2}cx_4 - \frac{1}{8}(2\alpha_2 - 3\alpha_3)\,x_3\left(x_3^2 + x_4^2\right) + \beta_2 x_3\left(x_1^2 + x_2^2\right). \tag{23d}$$

It is obviously known that Equations (23) has a trivial zero solution $(x_1, x_2, x_3, x_4) = (0, 0, 0, 0)$ at which the Jacobi matrix can be written as

$$J = D_x X = \begin{bmatrix} -\frac{1}{2}c & -(\sigma_1 + f_0) & 0 & 0 \\ (\sigma_1 - f_0) & -\frac{1}{2}c & 0 & 0 \\ 0 & 0 & -\frac{1}{2}c & -\frac{1}{2}\sigma_2 \\ 0 & 0 & \frac{1}{2}\sigma_2 & -\frac{1}{2}c \end{bmatrix}. \tag{24}$$

where $f_0 = \alpha_1 F_1$.

The characteristic equation corresponding to the trivial zero solution is of the form

$$\left(\lambda^2 + c\lambda + \frac{1}{4}c^2 + \sigma_1^2 - f_0^2\right)\left(\lambda^2 + c\lambda + \frac{1}{4}c^2 + \frac{1}{4}\sigma_2^2\right) = 0. \tag{25}$$

Let

$$\Delta_1 = \frac{1}{4}c^2 + \sigma_1^2 - f_0^2, \quad \Delta_2 = \frac{1}{4}\left(c^2 + \sigma_2^2\right). \tag{26}$$

When $c = 0$ and $\Delta_1 = \sigma_1^2 - f_0^2 = 0$ are simultaneously satisfied, system (23) has a double zero and a pair of pure imaginary eigenvalues

$$\lambda_{1,2} = 0, \quad \lambda_{3,4} = \pm i\bar{\omega}_2, \tag{27}$$

where $\bar{\omega}_2^2 = \sigma_2^2/4$.

Let $\sigma_1 = f_0 + \bar{\sigma}_1$ as well as set $f_0 = -1$. Considering $\bar{\sigma}_1$, c and f_2 as the perturbation parameters, then, averaged Equations (23) without the perturbation parameters is changed to the following form

$$\dot{x}_1 = x_2 + \frac{1}{16}(2\alpha_2 - 3\alpha_3)\,x_2\left(x_1^2 + x_2^2\right) - \beta_1 x_2\left(x_3^2 + x_4^2\right), \tag{28a}$$

$$\dot{x}_2 = -\frac{1}{16}(2\alpha_2 - 3\alpha_3)\,x_1\left(x_1^2 + x_2^2\right) + \beta_1 x_1\left(x_3^2 + x_4^2\right), \tag{28b}$$

$$\dot{x}_3 = -\frac{1}{2}\sigma_2 x_4 + \frac{1}{8}(2\alpha_2 - 3\alpha_3)\,x_4\left(x_3^2 + x_4^2\right) - \beta_2 x_4\left(x_1^2 + x_2^2\right), \tag{28c}$$

$$\dot{x}_4 = \frac{1}{2}\sigma_2 x_3 - \frac{1}{8}(2\alpha_2 - 3\alpha_3)\,x_3\left(x_3^2 + x_4^2\right) + \beta_2 x_3\left(x_1^2 + x_2^2\right). \tag{28d}$$

In the case considered here, we have

$$A = \begin{pmatrix} 0 & 1 & 0 & 0 \\ 0 & 0 & 0 & 0 \\ 0 & 0 & 0 & -\frac{1}{2}\sigma_2 \\ 0 & 0 & \frac{1}{2}\sigma_2 & 0 \end{pmatrix}. \tag{29}$$

Executing the Maple program given by Zhang et al. [39], the three-order normal form of system (28) is obtained as

$$\dot{y}_1 = y_2, \tag{30a}$$
$$\dot{y}_2 = -\left(\frac{1}{8}\alpha_2 - \frac{3}{16}\alpha_3\right) y_1^3 + \beta_1 y_1 y_3^2 + \beta_1 y_1 y_4^2, \tag{30b}$$
$$\dot{y}_3 = -\frac{1}{2}\sigma_2 y_4 + \left(\frac{1}{4}\alpha_2 - \frac{3}{8}\alpha_3\right) y_4^3 - \beta_2 y_1^2 y_4 + \left(\frac{1}{4}\alpha_2 - \frac{3}{8}\alpha_3\right) y_3^2 y_4, \tag{30c}$$
$$\dot{y}_4 = \frac{1}{2}\sigma_2 y_3 - \left(\frac{1}{4}\alpha_2 - \frac{3}{8}\alpha_3\right) y_3^3 + \beta_2 y_1^2 y_3 - \left(\frac{1}{4}\alpha_2 - \frac{3}{8}\alpha_3\right) y_3 y_4^2. \tag{30d}$$

The nonlinear transformation used here is given as follows

$$x_1 = y_1 + \left(\frac{1}{48}\alpha_2 - \frac{1}{32}\alpha_3\right) y_1^3 + \left(\frac{1}{8}\alpha_2 - \frac{3}{16}\alpha_3\right) y_1 y_2^2 - \beta_1 y_1 y_3^2 - \beta_1 y_1 y_4^2, \tag{31a}$$
$$x_2 = y_2 - \left(\frac{1}{16}\alpha_2 - \frac{3}{32}\alpha_3\right) y_1 y_2^2, \tag{31b}$$
$$x_3 = y_3 - \beta_2 y_1 y_2 y_4, \tag{31c}$$
$$x_4 = y_4 + \beta_2 y_1 y_2 y_3. \tag{31d}$$

The normal form with parameters can be written as

$$\dot{y}_1 = -\bar{\mu} y_1 + (1 - \sigma_1) y_2, \tag{32a}$$
$$\dot{y}_2 = \bar{\sigma}_1 y_1 - \bar{\mu} y_2 - \left(\frac{1}{8}\alpha_2 - \frac{3}{16}\alpha_3\right) y_1^3 + \beta_1 y_1 y_3^2 + \beta_1 y_1 y_4^2, \tag{32b}$$
$$\dot{y}_3 = -\bar{\mu} y_3 - \bar{\sigma}_2 y_4 + \left(\frac{1}{4}\alpha_2 - \frac{3}{8}\alpha_3\right) y_4^3 - \beta_2 y_1^2 y_4 + \left(\frac{1}{4}\alpha_2 - \frac{3}{8}\alpha_3\right) y_3^2 y_4, \tag{32c}$$
$$\dot{y}_4 = -\bar{f}_2 + \bar{\sigma}_2 y_3 - \bar{\mu} y_4 - \left(\frac{1}{4}\alpha_2 - \frac{3}{8}\alpha_3\right) y_3^3 + \beta_2 y_1^2 y_3 - \left(\frac{1}{4}\alpha_2 - \frac{3}{8}\alpha_3\right) y_3 y_4^2, \tag{32d}$$

where $\bar{\mu} = \frac{1}{2}c$, $\bar{\sigma}_2 = \frac{1}{2}\sigma_2$ and $\bar{f}_2 = \frac{1}{2}f_2$.

The results obtained above completely agree with those presented by using the direct method developed in [40].

Further, we let

$$y_3 = I\cos\gamma \quad \text{and} \quad y_4 = I\sin\gamma. \tag{33}$$

Substituting Equation (33) into Equation (32) yields

$$\dot{y}_1 = -\bar{\mu} y_1 + (1 - \bar{\sigma}_1) y_2, \tag{34a}$$

$$\dot{y}_2 = \bar{\sigma}_1 y_1 - \bar{\mu} y_2 - \left(\frac{1}{8}\alpha_2 - \frac{3}{16}\alpha_3\right) y_1^3 + \beta_1 y_1 I^2, \tag{34b}$$

$$\dot{I} = -\bar{\mu} I - \bar{f}_2 \sin\gamma, \tag{34c}$$

$$I\dot{\gamma} = \bar{\sigma}_2 I - \left(\frac{1}{4}\alpha_2 - \frac{3}{8}\alpha_3\right) I^3 + \beta_2 I y_1^2 - \bar{f}_2 \cos\gamma. \tag{34d}$$

In order to obtain the unfolding of Equations (34), a linear transformation is introduced as

$$\begin{bmatrix} y_1 \\ y_2 \end{bmatrix} = \frac{\sqrt{|\beta_1|}}{\sqrt{|\beta_2|}} \begin{bmatrix} 1 - \bar{\sigma}_1 & 0 \\ \bar{\mu} & 1 \end{bmatrix} \begin{bmatrix} u_1 \\ u_2 \end{bmatrix}. \tag{35}$$

Then, we have

$$\begin{bmatrix} u_1 \\ u_2 \end{bmatrix} = \frac{\sqrt{|\beta_2|}}{\sqrt{|\beta_1|}(1 - \bar{\sigma}_1)} \begin{bmatrix} 1 & 0 \\ -\bar{\mu} & 1 - \bar{\sigma}_1 \end{bmatrix} \begin{bmatrix} y_1 \\ y_2 \end{bmatrix}. \tag{36}$$

Substituting Equations (35) and (36) into Equation (34) and canceling the nonlinear terms which include the parameter $\bar{\sigma}_1$ yield the unfolding as

$$\dot{u}_1 = u_2, \tag{37a}$$

$$\dot{u}_2 = -\mu_1 u_1 - \mu_2 u_2 + \eta_1 u_1^3 + \beta_1 u_1 I^2, \tag{37b}$$

$$\dot{I} = -\bar{\mu} I - \bar{f}_2 \sin\gamma, \tag{37c}$$

$$I\dot{\gamma} = \bar{\sigma}_2 I - \eta_2 I^3 + \beta_1 I u_1^2 - \bar{f}_2 \cos\gamma, \tag{37d}$$

where $\mu_1 = \bar{\mu}^2 - \bar{\sigma}_1(1 - \bar{\sigma}_1)$, $\mu_2 = 2\bar{\mu}$, $\eta_1 = \frac{|\beta_1|}{|\beta_2|}(\frac{3}{16}\alpha_3 - \frac{1}{8}\alpha_2)$ and $\eta_2 = (\frac{1}{4}\alpha_2 - \frac{3}{8}\alpha_3)$.

The following scale transformations is introduced

$$\mu_2 \to \varepsilon\mu_2, \quad \bar{\mu} \to \varepsilon\bar{\mu}, \quad \bar{f}_2 \to \varepsilon\bar{f}_2, \quad \eta_1 \to \varepsilon\eta_1, \quad \eta_2 \to \eta_2. \tag{38}$$

Then, unfolding (37) can be rewritten as the Hamiltonian form with the perturbation

$$\dot{u}_1 = \frac{\partial H}{\partial u_2} + \varepsilon g^{u_1} = u_2, \tag{39a}$$

$$\dot{u}_2 = -\frac{\partial H}{\partial u_1} + \varepsilon g^{u_2} = -\mu_1 u_1 + \eta_1 u_1^3 + \beta_1 u_1 I^2 - \varepsilon\mu_2 u_2, \tag{39b}$$

$$\dot{I} = \frac{\partial H}{\partial \gamma} + \varepsilon g^{I} = -\varepsilon\bar{\mu} I - \varepsilon\bar{f}_2 \sin\gamma, \tag{39c}$$

$$I\dot{\gamma} = -\frac{\partial H}{\partial I} + \varepsilon g^{\gamma} = \bar{\sigma}_2 I - \eta_2 I^3 + \beta_1 I u_1^2 - \varepsilon\bar{f}_2 \cos\gamma, \tag{39d}$$

where the Hamiltonian function is of the form

$$H(u_1, u_2, I, \gamma) = \frac{1}{2}u_2^2 + \frac{1}{2}\mu_1 u_1^2 - \frac{1}{4}\eta_1 u_1^4 - \frac{1}{2}\beta_1 I^2 u_1^2 - \frac{1}{2}\bar{\sigma}_2 I^2 + \frac{1}{4}\eta_2 I^4, \tag{40}$$

and $g^{u_1} = 0$, $g^{u_2} = -\mu_2 u_2$, $g^{I} = -\bar{\mu} I - \bar{f}_2 \sin\gamma$, $g^{\gamma} = -\bar{f}_2 \cos\gamma$.

4. Dynamics of the Decoupled System

When $\varepsilon = 0$, it is seen that system (39) is an uncoupled two-degree-of-freedom nonlinear system. The variable I appears in components (u_1, u_2) of system (39) as a parameter since $\dot{I} = 0$. Consider the first two decoupled equations with perturbation term

$$\dot{u}_1 = \frac{\partial H}{\partial u_2} + \varepsilon g^{u_1} = u_2, \tag{41a}$$

$$\dot{u}_2 = -\frac{\partial H}{\partial u_1} + \varepsilon g^{u_2} = -\mu_1 u_1 + \eta_1 u_1^3 + \beta_1 u_1 I^2 - \varepsilon \mu_2 u_2. \tag{41b}$$

Assuming $\eta_1 > 0$, system (41) can exhibit the heteroclinic bifurcations in plane (u_1, u_2). It is easy to see from Equation (41) that when $\beta_1 I^2 - \mu_1 > 0$, the only solution of system (41) is the trivial zero solution $(u_1, u_2) = (0, 0)$ which is the saddle point. On the curve defined by $\mu_1 = \beta_1 I^2$, that is,

$$\bar{\mu}^2 = \bar{\sigma}_1(1 - \bar{\sigma}_1) + \beta_1 I^2, \tag{42}$$

or

$$I_{1,2} = \pm \left[\frac{\bar{\mu}^2 - \bar{\sigma}_1 (1 - \bar{\sigma}_1)}{\beta_1} \right]^{1/2}, \tag{43}$$

the trivial zero solution may bifurcate into three solutions through a pitchfork bifurcation represented by $q_0 = (0, 0)$ and $q_\pm(I) = (B, 0)$, respectively, where

$$B = \pm \left\{ \frac{1}{\eta_1} [\bar{\mu}^2 - \bar{\sigma}_1(1 - \bar{\sigma}_1) - \beta_1 I^2] \right\}^{1/2}. \tag{44}$$

From the Jacobian matrix evaluated at the nonzero solutions $q_\pm(I)$, it is found that the singular points $q_\pm(I)$ are the saddle points. On the line $\mu_2 = 0$, the Hopf bifurcation can occur from the trivial zero solution. The simple analysis for the Hopf bifurcation indicates that when $\mu_2 < 0$, the limit cycle is stable. The diagram of pitchfork bifurcation is shown in Figure 2.

It is observed that variables I and γ may actually represent the amplitude and phase of nonlinear oscillations. Therefore, we may assume that variable $I \geq 0$ and Equation (43) becomes

$$I_1 = 0, \quad I_2 = \left[\frac{\bar{\mu}^2 - \bar{\sigma}_1 (1 - \bar{\sigma}_1)}{\beta_1} \right]^{1/2}, \tag{45}$$

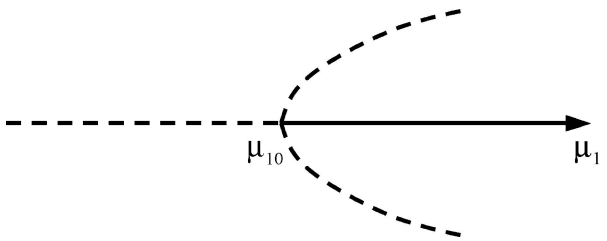

Figure 2. Pitchfork bifurcation in Equation (41).

such that for all $I \in [I_1,\ I_2]$, system (41) has two hyperbolic saddle points, $q_\pm(I)$, which are connected by a pair of heteroclinic orbits, $u^h_\pm(T_1,\ I)$, that is, $\lim_{T_1\to\pm\infty} u^h_\pm(T_1,\ I) = q_\pm(I)$. Therefore, in full four-dimensional phase space the set defined by

$$M = \{(u,\ I,\ \gamma) \mid u = q_\pm(I), I_1 \le I \le I_2, 0 \le \gamma < 2\pi\} \tag{46}$$

is a two-dimensional invariant manifold. It is known that two-dimensional invariant manifold M is normally hyperbolic. Two-dimensional, normally hyperbolic and invariant manifold M has three-dimensional stable and unstable manifolds which are respectively expressed as $W^s(M)$ and $W^u(M)$. The existence of the heteroclinic orbit of system (41) to the saddle points $q_\pm(I) = (B,\ 0)$ indicates that the stable and unstable manifolds $W^s(M)$ and $W^u(M)$ intersect nontransversally along a three-dimensional heteroclinic manifold denoted by Γ, which can be written as

$$\Gamma = \left\{ (u,\ I,\ \gamma) \,\middle|\, u = u^h_\pm(T_1,\ I),\ I_1 < I < I_2,\ \gamma = \int_0^{T_1} D_I H\big(u^h_\pm(T_1,\ I),\ I\big)\, ds + \gamma_0 \right\}. \tag{47}$$

Now we analyze the dynamics of the unperturbed system of Equation (39) restricted to the manifold M. Considering the unperturbed system of (39) restricted to the manifold M yields

$$\begin{aligned} \dot{I} &= 0, \\ I\dot{\gamma} &= D_I H(q_\pm(I),\ I), \quad I_1 \le I \le I_2, \end{aligned} \tag{48}$$

where

$$D_I H\,(q_\pm(I),\ I) = -\frac{\partial H\,(q_\pm(I),\ I)}{\partial I} = \bar{\sigma}_2 I - \eta_2 I^3 + \beta_1 I q^2_\pm\,(I)\,. \tag{49}$$

Based on the analysis given by Kovacic and Wiggins in [18], it is known that if the condition $D_I H(q_\pm(I),\ I) \neq 0$ is satisfied, $I =$ constant is called as a periodic orbit and if the condition $D_I H(q_\pm(I),\ I) = 0$ is satisfied, $I =$ constant is called as a circle of the singular points. A value of $I \in [I_1,\ I_2]$ at which $D_I H(q_\pm(I),\ I) = 0$ is referred to as a resonant I value and these singular points as the resonant singular points. We denote a resonant value by I_r so that

$$D_I H\,(q_\pm(I),\ I) = \bar{\sigma}_2 I_r - \eta_2 I_r^3 + \frac{\beta_1 I_r}{\eta_1}\left[\bar{\mu}^2 - \bar{\sigma}_1\,(1 - \bar{\sigma}_1) - \beta_1 I_r^2\right] = 0. \tag{50}$$

Then, we obtain a resonant value

$$I_r = \pm\left\{ \frac{\eta_1\bar{\sigma}_2 + \beta_1[\bar{\mu}^2 - \bar{\sigma}_1\,(1 - \bar{\sigma}_1)]}{\eta_1\eta_2 + \beta_1^2} \right\}^{1/2}. \tag{51}$$

The geometry structure of the stable and unstable manifolds of M in full four-dimensional phase space for the unperturbed system of (39) is given in Figure 3. Because variable γ may represent the phase of nonlinear oscillations, when $I = I_r$, the phase shift $\Delta\gamma$ of nonlinear oscillations is defined as

$$\Delta\gamma = \gamma(+\infty,\ I_r) - \gamma(-\infty,\ I_r). \tag{52}$$

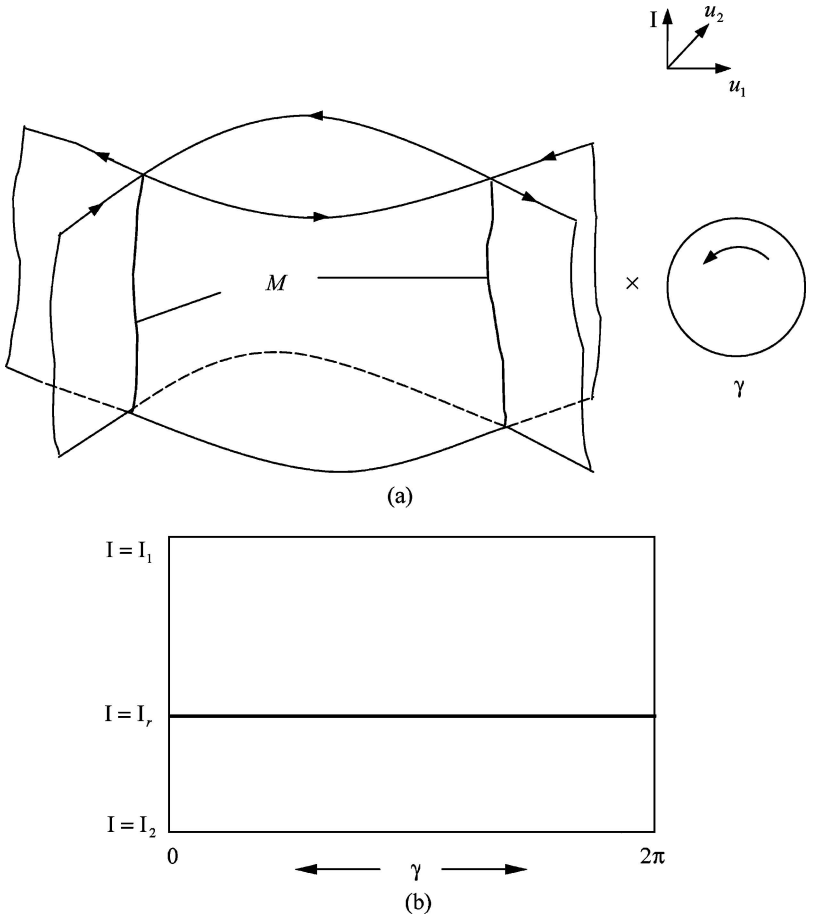

Figure 3. The geometric structure of manifolds M, $W^s(M)$ and $W^u(M)$ in full four-dimensional phase space.

The physical interpretation of the phase shift is the phase difference between the two end points of the orbit. In (u_1, u_2) subspace, there exist a pair of the heteroclinic orbits connecting the two saddles. Therefore, the homoclinic orbit in subspace (I, γ) is of a heteroclinic connecting in full four-dimensional phase space (u_1, u_2, I, γ). The phase shift represents the difference of γ value as a trajectory leaves and returns to the basin of attraction of the manifold M. We will use the phase shift in subsequent analysis to obtain the condition for the existence of the Silnikov type single-pulse homoclinic orbit. The phase shift will be calculated in the later analysis for the heteroclinic orbit.

Now we consider the heteroclinic bifurcations of Equation (41). Letting $\varepsilon_1 = \mu_1 - \beta_1 I^2$ and $\varepsilon_2 = \mu_2$, Equation (41) can be rewritten as

$$\begin{aligned} \dot{u}_1 &= u_2, \\ \dot{u}_2 &= -\varepsilon_1 u_1 + \eta_1 u_1^3 - \varepsilon\varepsilon_2 u_2. \end{aligned} \tag{53}$$

Setting $\varepsilon = 0$ in Equation (53), it is seen that Equation (53) is a Hamiltonian system with Hamiltonian function

$$H(u_1, u_2) = \frac{1}{2}u_2^2 + \frac{1}{2}\varepsilon_1 u_1^2 - \frac{1}{4}\eta_1 u_1^4. \tag{54}$$

When $H = \varepsilon_1^2/4\eta_1$, there exists a heteroclinic loop Γ^0, which consists of the two hyperbolic saddles $q_\pm$ and a pair of heteroclinic orbits $u_\pm(T_1)$. The equations of a pair of heteroclinic orbits are obtained as

$$\begin{aligned} u_1(T_1) &= \pm\sqrt{\frac{\varepsilon_1}{\eta_1}}\tanh\left(\frac{\sqrt{2\varepsilon_1}}{2}T_1\right), \\ u_2(T_1) &= \pm\frac{\varepsilon_1}{\sqrt{2\eta_1}}\operatorname{sech}^2\left(\frac{\sqrt{2\varepsilon_1}}{2}T_1\right). \end{aligned} \tag{55}$$

The Melnikov function for the heteroclinic orbits is easily presented by

$$M(\varepsilon_1, \varepsilon_2, I) = \int_{-\infty}^{\infty} u_2(T_1)\,[-\varepsilon_2 u_2(T_1)]\,d\,T_1 = -\frac{2\sqrt{2}\varepsilon_1^{3/2}\varepsilon_2}{3\eta_1}. \tag{56}$$

To keep the heteroclinic loop preserved under a perturbation, it is necessary to require that $M(\varepsilon_1, \varepsilon_2, I) = 0$. Therefore, Equation (56) leads to $\varepsilon_1 = 0$ or $\varepsilon_2 = 0$. When we choose $\varepsilon_1 = 0$, that is, $\bar{\mu}^2 - \bar{\sigma}_1(1 - \bar{\sigma}_1) = \beta_1 I^2$, it is known from the aforementioned analysis that the curve $\bar{\mu}^2 - \bar{\sigma}_1(1 - \bar{\sigma}_1) = \beta_1 I^2$ is a curve for the pitchfork bifurcation. There exist the two saddle points $q_\pm(I) = (B, 0)$ when the condition $\bar{\mu}^2 - \bar{\sigma}_1(1 - \bar{\sigma}_1) > \beta_1 I^2$ is only satisfied. Therefore, on the curve $\varepsilon_1 = 0$ the heteroclinic loop does not exist. Choosing $\varepsilon_2 = 0$, a heteroclinic bifurcation curve is obtained as

$$\bar{\mu} = 0, \quad \bar{\mu}^2 - \bar{\sigma}_1(1 - \bar{\sigma}_1) > \beta_1 I^2. \tag{57}$$

Based on Equations (42) and (57), the bifurcation diagram of system (41) is given in Figure 4, and the corresponding phase portraits are obtained in Figure 5. It is observed that the bifurcation set may be divided into four different regions. When the parameters are located in the same region, the phase portraits of system (41) are of the same topological structures.

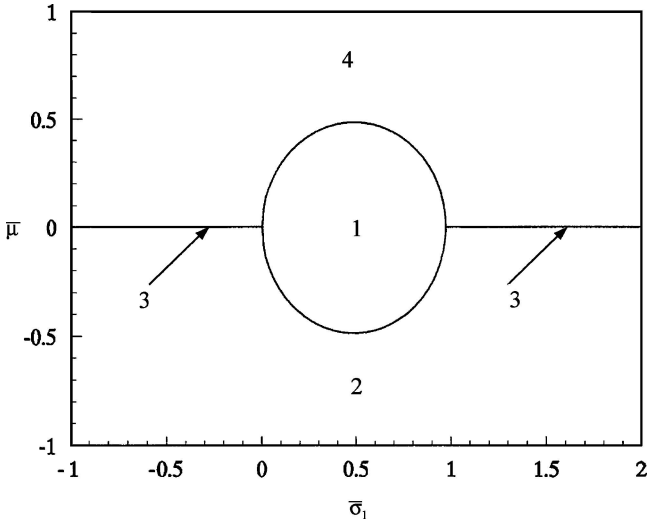

Figure 4. The bifurcation set of system (41): (1) saddle point; (2) heteroclinic orbit and stable limit cycle; (3) heteroclinic loop; (4) heteroclinic orbit and unstable limit cycle.

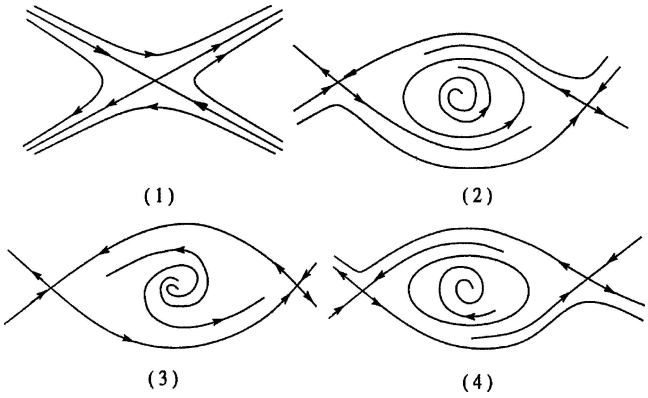

Figure 5. The phase portraits in the different regions.

In the following study, the computation of the phase shift is considered. Substituting the first equation of (55) into the fourth equation of the unperturbed system of Equation (39) yields

$$\dot{\gamma} = \bar{\sigma}_2 - \eta_2 I^2 + \frac{\varepsilon_1 \beta_1}{\eta_1} \tanh^2 \left(\frac{\sqrt{2\varepsilon_1}}{2} T_1 \right). \tag{58}$$

Integrating Equation (58) yields

$$\gamma(T_1) = \omega_r T_1 - \frac{\beta_1 \sqrt{2\varepsilon_1}}{\eta_1} \tanh \left(\frac{\sqrt{2\varepsilon_1}}{2} T_1 \right) + \gamma_0, \tag{59}$$

where

$$\omega_r = \bar{\sigma}_2 - \eta_2 I^2 + \frac{\varepsilon_1 \beta_1}{\eta_1}. \tag{60}$$

At $I = I_r$, there is $\omega_r \equiv 0$. Therefore, the phase shift is expressed as

$$\Delta\gamma = \left[-\frac{2\beta_1 \sqrt{2\varepsilon_1}}{\eta_1} \right]_{I=I_r} = -\frac{2\beta_1}{\eta_1} \sqrt{2\left[\bar{\mu}^2 - \bar{\sigma}_1 (1 - \bar{\sigma}_1) - \beta_1 I_r^2\right]}. \tag{61}$$

5. Global Analysis of Perturbed System

In this section, the dynamics of the perturbed system and the effect of small perturbations on the manifold M are analyzed. Based on the analysis in [17, 18], we know that the manifold M along with its stable and unstable manifolds are invariant under small, sufficiently differentiable perturbations. It is noticed that the singular points $q_\pm(I)$ may persist under small perturbations, in particular, $M \to M_\varepsilon$. Therefore, we obtain

$$M = M_\varepsilon = \{(u,\ I,\ \gamma) \mid u = q_\pm(I),\ I_1 \le I \le I_2,\ 0 \le \gamma < 2\pi\}. \tag{62}$$

Considering the later two equations of (39) yields

$$\begin{aligned}\dot{I} &= -\bar{\mu} I - \bar{f}_2 I \sin\gamma,\\ \dot{\gamma} &= \bar{\sigma}_2 - \eta_2 I^2 + \beta_1 u_1^2 + \frac{\bar{f}_2}{I}\cos\gamma.\end{aligned} \tag{63}$$

It is known from the aforementioned analysis that there is a pair of pure imaginary eigenvalues in Equation (63). Therefore, resonance can occur in system (63).

Also introduce the scale transformations

$$\bar{\mu} \to \varepsilon\bar{\mu}, \quad I = I_r + \sqrt{\varepsilon}h, \quad \bar{f}_{21} \to \varepsilon f_{21}, \quad T_1 \to \frac{T_1}{\sqrt{\varepsilon}}. \tag{64}$$

Substituting the above transformations into Equation (63) yields

$$\begin{aligned}\dot{h} &= -\bar{\mu} I_r - \bar{f}_2 \sin\gamma - \sqrt{\varepsilon}\bar{\mu}h,\\ \dot{\gamma} &= -\frac{2\delta}{\eta_1} I_r h - \sqrt{\varepsilon}\left(\frac{\bar{f}_2}{I_r}\cos\gamma + \frac{\delta}{\eta_1}h^2\right),\end{aligned} \tag{65}$$

where $\delta = \eta_1\eta_2 + \beta_1^2$.

When $\varepsilon = 0$, Equation (65) becomes

$$\begin{aligned}\dot{h} &= -\bar{\mu} I_r - \bar{f}_2 \sin\gamma,\\ \dot{\gamma} &= -\frac{2\delta}{\eta_1} I_r h.\end{aligned} \tag{66}$$

The unperturbed system (66) is a Hamiltonian system with Hamiltonian function

$$H(h,\ \gamma) = -\bar{\mu} I_r \gamma - \bar{f}_2 \cos\gamma + \frac{\delta}{\eta_1} I_r h^2. \tag{67}$$

The singular points of Equation (66) are given as

$$p_0 = (0,\ \gamma_c) = \left(0, -\arcsin\frac{\bar{\mu} I_r}{\bar{f}_2}\right) \quad \text{and} \quad q_0 = (0,\ \gamma_s) = \left(0,\ \pi - \arcsin\frac{\bar{\mu} I_r}{\bar{f}_2}\right). \tag{68}$$

Based on the characteristic equations evaluated at the two singular points p_0 and q_0, we can know the stabilities of these singular points. The Jacobian matrix of Equation (66) is of the form

$$J = \begin{bmatrix} 0 & -\bar{f}_2\cos\gamma \\ -\frac{2\delta}{\eta_1} I_r & 0 \end{bmatrix}. \tag{69}$$

The characteristic equation corresponding to the singular point p_0 is obtained as

$$\lambda^2 - \frac{2\delta}{\eta_1} I_r \bar{f}_2 \cos\gamma_c = 0. \tag{70}$$

When the condition $\frac{2\delta}{\eta_1} I_r \bar{f}_2 \cos\gamma_c < 0$ is satisfied, Equation (66) has a pair of pure imaginary eigenvalues. Therefore, it is known that the singular point p_0 is a center.

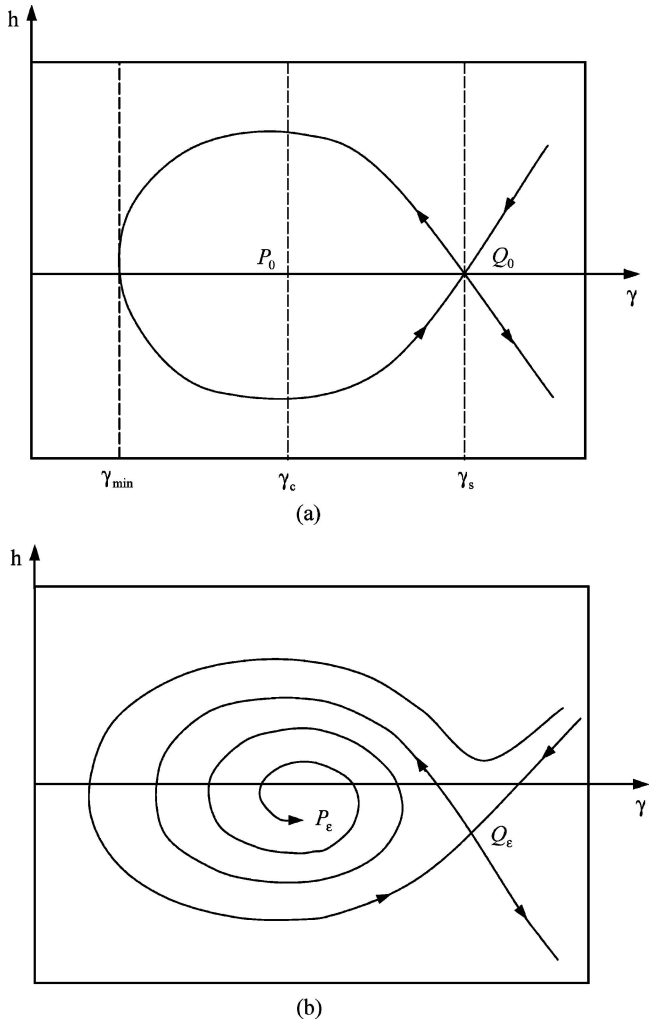

Figure 6. Dynamics on the normally hyperbolic manifold; (a) the unperturbed case; (b) the perturbed case.

The characteristic equation corresponding to the singular point q_0 is obtained as

$$\lambda^2 - \frac{2\delta}{\eta_1} I_r \bar{f}_2 \cos\gamma_s = 0. \tag{71}$$

When the condition $\frac{2\delta}{\eta_1} I_r \bar{f}_2 \cos\gamma_s > 0$ is satisfied, Equation (66) has two real, unequal and opposite sign eigenvalues. So, the singular point q_0 is a saddle, which is connected to itself by a homoclinic orbit. The phase portrait of Equation (66) is given in Figure 6(a).

It is found that for sufficiently small ε, the singular point q_0 remains a hyperbolic singular point q_ε of saddle stability type. From Equation (65), it is known that the Jacobian matrix of the linearization of Equation (65) is of the form

$$J_\varepsilon = \begin{bmatrix} -\sqrt{\varepsilon}\bar{\mu} & -f_2 \cos\gamma_c \\ -\frac{2\delta}{\alpha_1} I_r & \sqrt{\varepsilon}\frac{f_2}{I_r} \sin\gamma_c \end{bmatrix}. \tag{72}$$

or

$$J_{p_\varepsilon} = \begin{bmatrix} -\sqrt{\varepsilon}\bar{\mu} & -f_2 \cos\gamma_c \\ -\frac{2\delta}{\alpha_1} I_r & -\sqrt{\varepsilon}\bar{\mu} \end{bmatrix}. \tag{73}$$

Based on Equation (73), we find that the leading order term of the trace in the linearization of (65) is less than zero inside the homoclinic loop. Therefore, for the small perturbations, the singular point p_0 becomes a hyperbolic sink p_ε. The phase portrait of perturbed system (65) is also depicted in Figure 6(b).

At $h = 0$, the estimate of basin of attraction for $\gamma_{\min}$ is obtained as

$$\bar{\mu} I_r \gamma_{\min} + \bar{f}_2 \cos\gamma_{\min} = \bar{\mu} I_r \gamma_s + \bar{f}_2 \cos\gamma_s \tag{74}$$

Substituting γ_s in Equation (68) into Equation (74) yields

$$\gamma_{\min} + \frac{\bar{f}_2}{\bar{\mu} I_r} \cos\gamma_{\min} = \pi - \arcsin\frac{\bar{\mu} I_r}{\bar{f}_2} + \frac{\sqrt{\bar{f}_2^2 - \bar{\mu}^2 I_r^2}}{\bar{\mu} I_r}. \tag{75}$$

Define an annulus A_ε near $I = I_r$ as

$$A_\varepsilon = \{(u_1,\ u_2,\ I,\ \gamma)\,|\,u_1 = B,\ u_2 = 0, |I - I_r| < \sqrt{\varepsilon}C,\ \gamma \in T^1\} \tag{76}$$

where C is a constant, which is chosen sufficient large so that the unperturbed homoclinic orbit is enclosed within the annulus. It is noticed that three-dimensional stable and unstable manifolds of A_ε, denoted as $W^s(A_\varepsilon)$ and $W^u(A_\varepsilon)$, are subsets of $W^s(M_\varepsilon)$ and $W^u(M_\varepsilon)$, respectively. We will show that for the perturbed system, the saddle focus p_ε on A_ε has a homoclinic orbit which comes out of the annulus A_ε and can return to the annulus in full four-dimensional space, and eventually may give rise to the Silnikov type homoclinic loop, as shown in Figure 7.

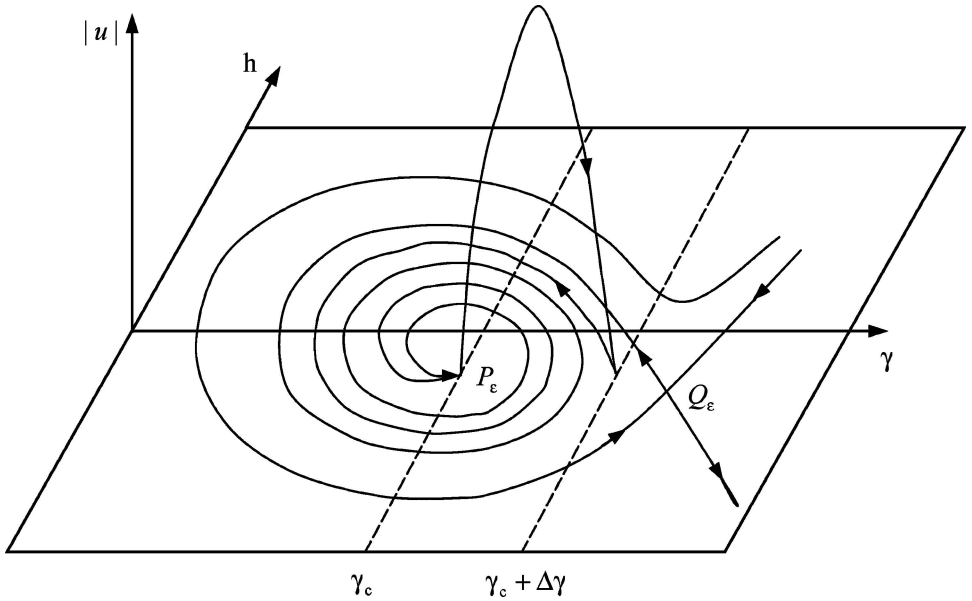

Figure 7. The Silnikov type single-pulse homoclinic orbit to saddle focus.

6. Higher-Dimensional Melnikov Theory

There are two steps to determine the existence of the Silnikov type single-pulse homoclinic orbit. In the first step, by using higher-dimensional Melnikov theory, the measure of the distance between one-dimensional unstable manifold $W^u(p_\varepsilon)$ and three-dimensional stable manifold $W^s(A_\varepsilon)$ may be obtained to show that $W^u(p_\varepsilon) \subset W^s(A_\varepsilon)$ when the Melnikov function has a simple zero. In the second step, it will be determined whether the orbit on $W^u(p_\varepsilon)$ comes back in the basin of attraction of A_ε. If it dose, the orbit will asymptote to A_ε as $t \to \infty$. If it does not, the orbit may escape from the annulus A_ε by crossing the boundary of the annulus.

Based on the results obtained in [18], higher-dimensional Melnikov function is given as follows

$$\begin{aligned} M\left(\mu_1,\, \bar{\sigma}_2,\, I_r,\, \bar{f}_2\right) &= \int_{-\infty}^{+\infty} \left[\frac{\partial H}{\partial u_1} g^{u_1} + \frac{\partial H}{\partial u_2} g^{u_2} + \frac{\partial H}{\partial I} g^{I} + \frac{\partial H}{\partial \gamma} g^{\gamma}\right] dT_1 \\ &= \int_{-\infty}^{+\infty} \left[-\mu_2 u_2^2\left(T_1\right) - \left(\bar{\sigma}_2 I_r - \eta_2 I_r^3 + \beta_1 I_r u_1^2\left(T_1\right)\right)\left(\bar{\mu} I_r + \bar{f}_2 \sin\gamma\left(T_1\right)\right)\right] dT_1, \end{aligned} \tag{77}$$

where $u_1(T_1)$, $u_2(T_1)$ and $\gamma(T_1)$ are respectively given in Equations (55) and (59).

From the aforementioned analysis, it is known that the first and second integrands are evaluated as follows

$$\int_{-\infty}^{+\infty} -\mu_2 u_2^2\left(T_1\right) dT_1 = -\frac{2\sqrt{2}\varepsilon_1^{3/2}\mu_2}{3\eta_1}, \tag{78}$$

and

$$\int_{-\infty}^{+\infty} \left[-\bar{\mu} I_r \left(\bar{\sigma}_2 I_r - \eta_2 I_r^3 + \beta_1 I_r u_1^2\left(T_1\right)\right)\right] dT_1 = -\bar{\mu} I_r^2 \Delta\gamma. \tag{79}$$

The third integral can be rewritten as

$$\begin{aligned} M_1\left(\mu_1,\, \bar{\sigma}_2,\, I_r,\, \bar{f}_2\right) &= -\bar{f}_2 I_r \int_{-\infty}^{+\infty} \sin\gamma\left(T_1\right)\left(\bar{\sigma}_2 - \eta_2 I_r^2 + \beta_1 u_1^2\left(T_1\right)\right) dT_1 \\ &= -\bar{f}_2 I_r \int_{-\infty}^{+\infty} \sin\gamma(T_1)\, d\left(\gamma(T_1)\right) = \bar{f}_2 I_r \left[\cos\gamma\left(+\infty\right) - \cos\gamma\left(-\infty\right)\right] \end{aligned} \tag{80}$$

Using $\Delta\gamma = \gamma(+\infty) - \gamma(-\infty)$ yields

$$M_1(\mu_1,\, \bar{\sigma}_2,\, I_r,\, \bar{f}_2) = \bar{f}_2 I_r[\cos\gamma(-\infty)(\cos\Delta\gamma - 1) - \sin\gamma(-\infty)\sin\Delta\gamma]. \tag{81}$$

Based on Equation (68), we have

$$\sin\gamma\left(-\infty\right) = -\frac{\bar{\mu} I_r}{\bar{f}_2}, \quad \cos\gamma\left(-\infty\right) = \frac{\sqrt{\bar{f}_2^2 - \bar{\mu}^2 I_r^2}}{\bar{f}_2}. \tag{82}$$

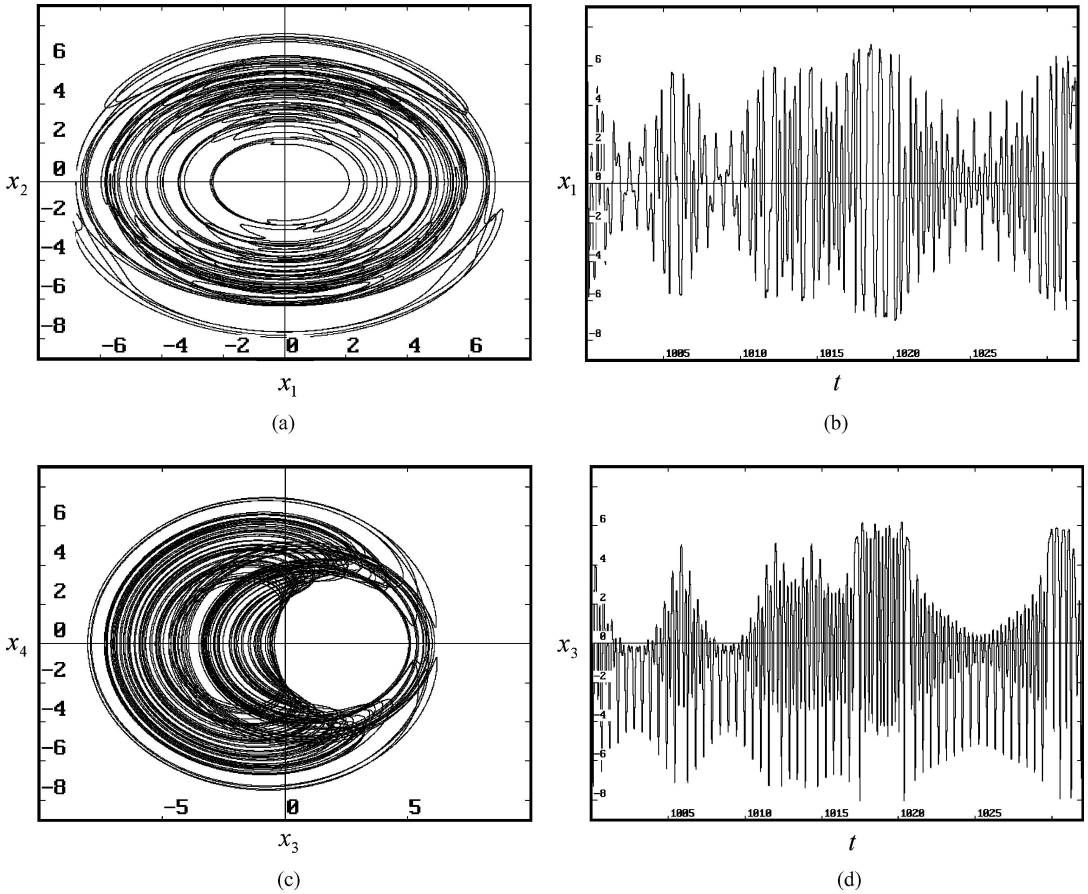

Figure 8. The chaotic responses in the nonlinear nonplanar oscillations of the cantilever beam subjected to a harmonic axial excitation and transverse excitations at the free end for $F_1 = 1.0$, $f_2 = 38.8$, $c = 0.011$, $\sigma_1 = 1.01$, $\sigma_2 = 1.5$, $\alpha_1 = 1$, $\alpha_2 = 13.2$, $\alpha_3 = 5.01$, $\beta_1 = 1.01$, $\beta_2 = 1.23$, $x_{10} = 5.055$, $x_{20} = -4.1385$, $x_{30} = 4.35$, $x_{40} = 3.18$; (a) the phase portrait on plane $(x_1,\ x_2)$; (b) the waveform on plane $(t,\ x_1)$; (c) phase portrait on plane $(x_3,\ x_4)$; (d) the waveform on plane $(t,\ x_3)$.

Substituting Equation (82) into Equation (81) yields

$$M_1(\mu_1,\ \bar{\sigma}_2,\ I_r,\ \bar{f}_2) = I_r\left[\sqrt{\bar{f}_2^2 - \bar{\mu}^2 I_r^2}(\cos\Delta\gamma - 1) + \bar{\mu} I_r \sin\Delta\gamma\right]. \tag{83}$$

Therefore, the Melnikov function is represented as

$$\begin{aligned} M\left(\mu_1,\ \bar{\sigma}_2,\ I_r,\ \bar{f}_2\right) = &-\frac{4\sqrt{2}\left[\bar{\mu}^2 - \bar{\sigma}_1\left(1 - \bar{\sigma}_1\right) - \beta_1 I_r^2\right]^{3/2}\bar{\mu}}{3\eta_1} - \bar{\mu} I_r^2 \Delta\gamma \\ &+ I_r\left[\sqrt{\bar{f}_2^2 - \bar{\mu}^2 I_r^2}\,(\cos\Delta\gamma - 1) + \bar{\mu} I_r \sin\Delta\gamma\right]. \end{aligned} \tag{84}$$

In order to determine the existence of the Silnikov type single-pulse homoclinic orbit, we first require that the Melnikov function must have a simple zero. Thus, the following expression is

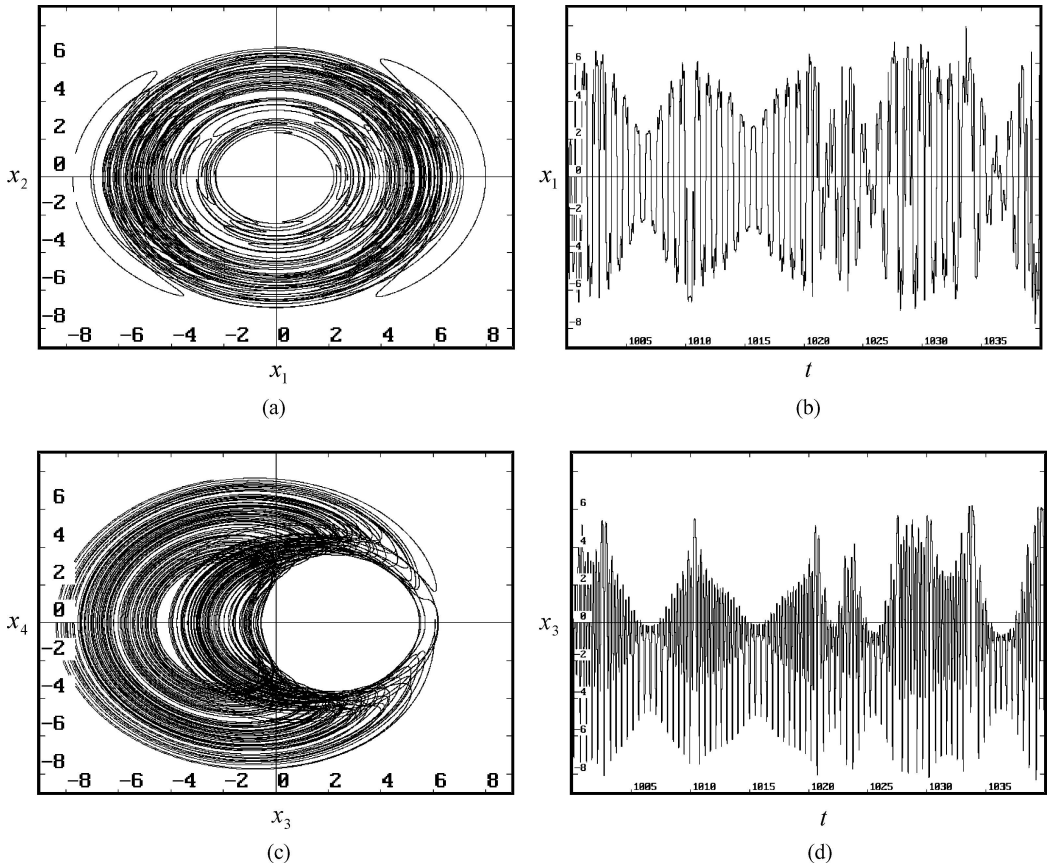

Figure 9. The chaotic responses in the nonlinear nonplanar oscillations of the cantilever beam for $F_1 = 1.0$, $f_2 = 43.8$, $c = 0.011$, $\sigma_1 = 1.01$, $\sigma_2 = 1.5$, $\alpha_1 = -1$, $\alpha_2 = 13.2$, $\alpha_3 = 5.01$, $\beta_1 = 1.01$, $\beta_2 = 1.23$, $x_{10} = 5.055$, $x_{20} = -4.1385$, $x_{30} = 4.35$, $x_{40} = 3.18$; (a) the phase portrait on plane $(x_1,\ x_2)$; (b) the waveform on plane $(t,\ x_1)$; (c) phase portrait on plane $(x_3,\ x_4)$; (d) the waveform on plane $(t,\ x_3)$.

obtained

$$\frac{4\sqrt{2}\left[\bar{\mu}^2 - \bar{\sigma}_1(1-\bar{\sigma}_1) - \beta_1 I_r^2\right]^{3/2}\bar{\mu}}{3\eta_1} + \bar{\mu} I_r^2 \Delta\gamma - I_r\left\lfloor\sqrt{\bar{f}_2^2 - \bar{\mu}^2 I_r^2}\,(\cos\Delta\gamma - 1) - \bar{\mu} I_r \sin\Delta\gamma\right\rfloor = 0. \tag{85}$$

Next, we determine whether the orbit on $W^u(p_\varepsilon)$ returns to the basin of attraction of A_ε. The condition is given as

$$\gamma_{\min} < \gamma_c + \Delta\gamma + m\pi < \gamma_s, \tag{86}$$

where m is an integer, $\Delta\gamma$, γ_c, γ_s and $\gamma_{\min}$ are respectively given by Equations (61), (68) and (75). It indicates that $W^u(p_\varepsilon) \subset W^s(A_\varepsilon)$, that is, one-dimensional unstable manifold $W^u(p_\varepsilon)$ is a subset of three-dimensional stable manifold $W^s(A_\varepsilon)$. When the conditions (85) and (86) are simultaneously

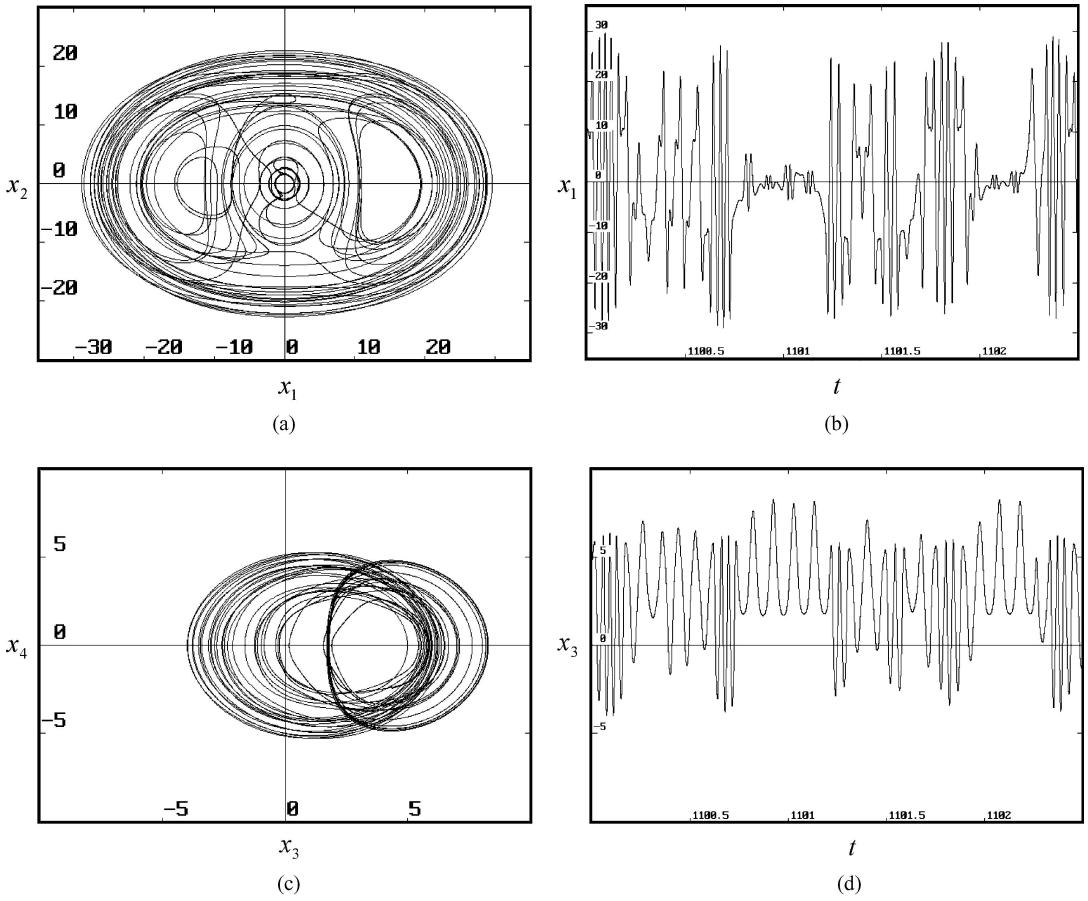

Figure 10. The chaotic responses in the nonlinear nonplanar oscillations of the cantilever beam for $F_1 = 49.7$, $f_{21} = 416.8$, $c = 0.1$, $\sigma_1 = 2.0$, $\sigma_2 = 6.5$, $\alpha_1 = 1$, $\alpha_2 = -4.2$, $\alpha_3 = 0.01$, $\beta_1 = -5.1$, $\beta_2 = 0.23$, $x_{10} = 0.1385$, $x_{20} = 0.055$, $x_{30} = 0.35$, $x_{40} = 0.18$; (a) the phase portrait on plane $(x_1,\ x_2)$; (b) the waveform on plane $(t,\ x_1)$; (c) phase portrait on plane $(x_3,\ x_4)$; (d) the waveform on plane (t, x_3).

satisfied, it is shown that there exists the Silnikov type single-pulse chaos in system (39), that is, system (39) may give rise to chaotic motions in the sense of the Smale horseshoes.

7. Numerical Simulation of Chaotic Motions

We choose averaged Equation (22) to do numerical simulations because the global perturbation method given by Kovacic and Wiggins in [18] can be only used to analyze the autonomous systems but can not be used to analyze the non-autonomous systems. In addition, it is not known up to now how to express the phase portraits or the topological structures of higher dimensional non-autonomous systems in high-dimensional space. In this section, numerical approach through a computer software *Dynamics* [41] is utilized to explore the existence of the chaotic motions in the nonlinear nonplanar oscillations of the cantilever beam subjected to a harmonic axial excitation and transverse excitations at the free end.

Figure 8 demonstrates the existence of the chaotic response in the nonlinear nonplanar oscillations of the cantilever beam for the parametric excitation $F_1 = 1.0$ and the forcing excitation $f_2 = 38.8$. Other

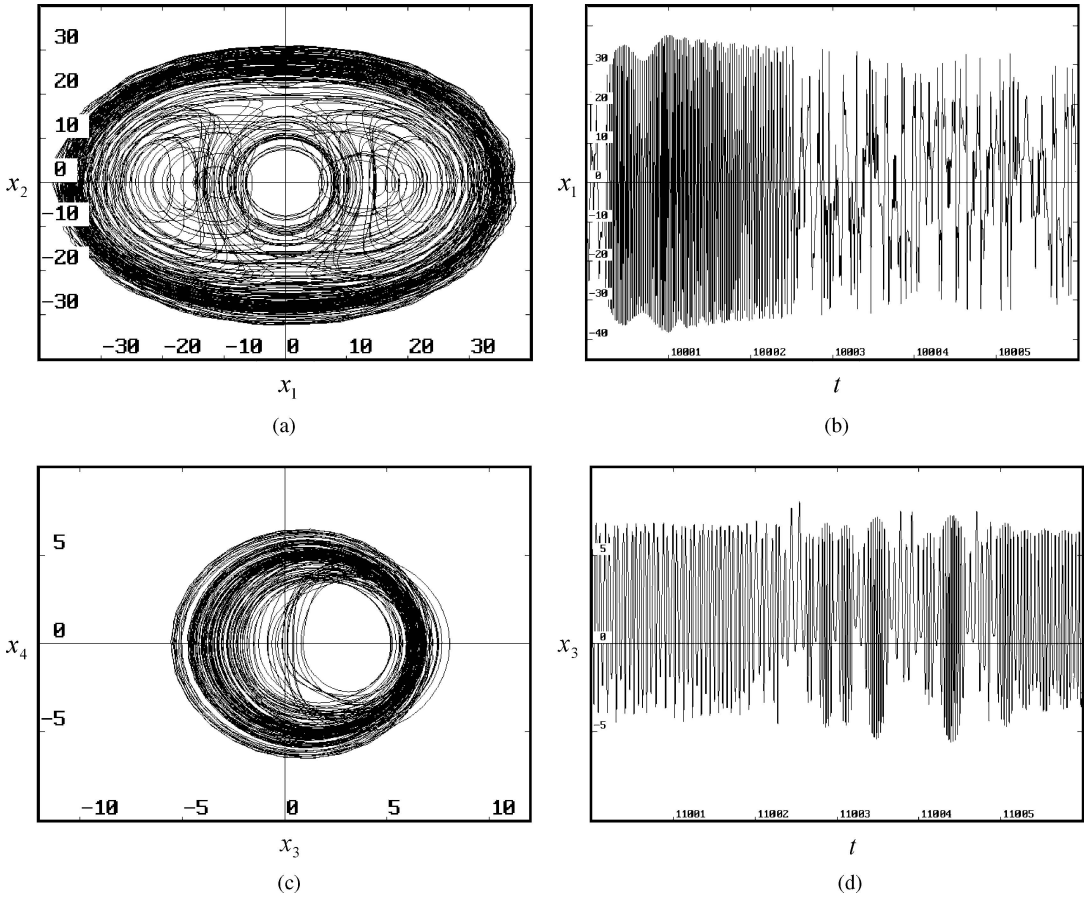

Figure 11. The chaotic responses in the nonlinear nonplanar oscillations of the cantilever beam for $F_1 = 61.7$, $f_2 = 416.8$, $c = 0.11$, $\sigma_1 = 2.0$, $\sigma_2 = 6.5$, $\alpha_1 = 1$, $\alpha_2 = -4.2$, $\alpha_3 = 0.01$, $\beta_1 = -5.1$, $\beta_2 = 0.23$, $x_{10} = 0.1385$, $x_{20} = 0.055$, $x_{30} = 0.35$, $x_{40} = 0.18$; (a) the phase portrait on plane $(x_1,\ x_2)$; (b) the waveform on plane $(t,\ x_1)$; (c) phase portrait on plane $(x_3,\ x_4)$; (d) the waveform on plane $(t,\ x_3)$.

parameters and initial conditions are chosen as $c = 0.011$, $\sigma_1 = 1.01$, $\sigma_2 = 1.5$, $\alpha_1 = 1$, $\alpha_2 = 13.2$, $\alpha_3 = 5.01$, $\beta_1 = 1.01$, $\beta_2 = 1.23$, $x_{10} = 5.055$, $x_{20} = -4.1385$, $x_{30} = 4.35$, $x_{40} = 3.18$, where c is linear damping coefficient, σ_1 and σ_2 are two detuning parameters. Figure 8(a)–8(d), respectively, represent the phase portraits on the planes $(x_1,\ x_2)$, $(x_3,\ x_4)$ and the waveforms on the planes $(t,\ x_1)$, $(t,\ x_3)$. In Figure 9, the chaotic motion occurs when transverse excitation in the z-direction and parameter α_1, respectively, are $f_2 = 43.8$ and $\alpha_1 = -1.0$. In this case, the chosen parameters and initial conditions are the same as those in Figure 8. In the aforementioned two cases, it is found that there exists a large difference between the phase portrait on the plane $(x_1,\ x_2)$ and the phase portrait on the plane $(x_3,\ x_4)$.

Figure 10 indicates that the chaotic response of the cantilever beam occurs when the parametric excitation, transverse excitation in the z-direction, parameters and initial conditions, respectively, are $F_1 = 49.7$, $f_2 = 416.8$, $c = 0.1$, $\sigma_1 = 2.0$, $\sigma_2 = 6.5$, $\alpha_1 = 1$, $\alpha_2 = -4.2$, $\alpha_3 = 0.01$, $\beta_1 = -5.1$, $\beta_2 = 0.23$, $x_{10} = 0.1385$, $x_{20} = 0.055$, $x_{30} = 0.35$, $x_{40} = 0.18$. When the parametric excitation and damping coefficient simultaneously change to $F_1 = 61.7$, $c = 0.11$, the chaotic motion of the cantilever

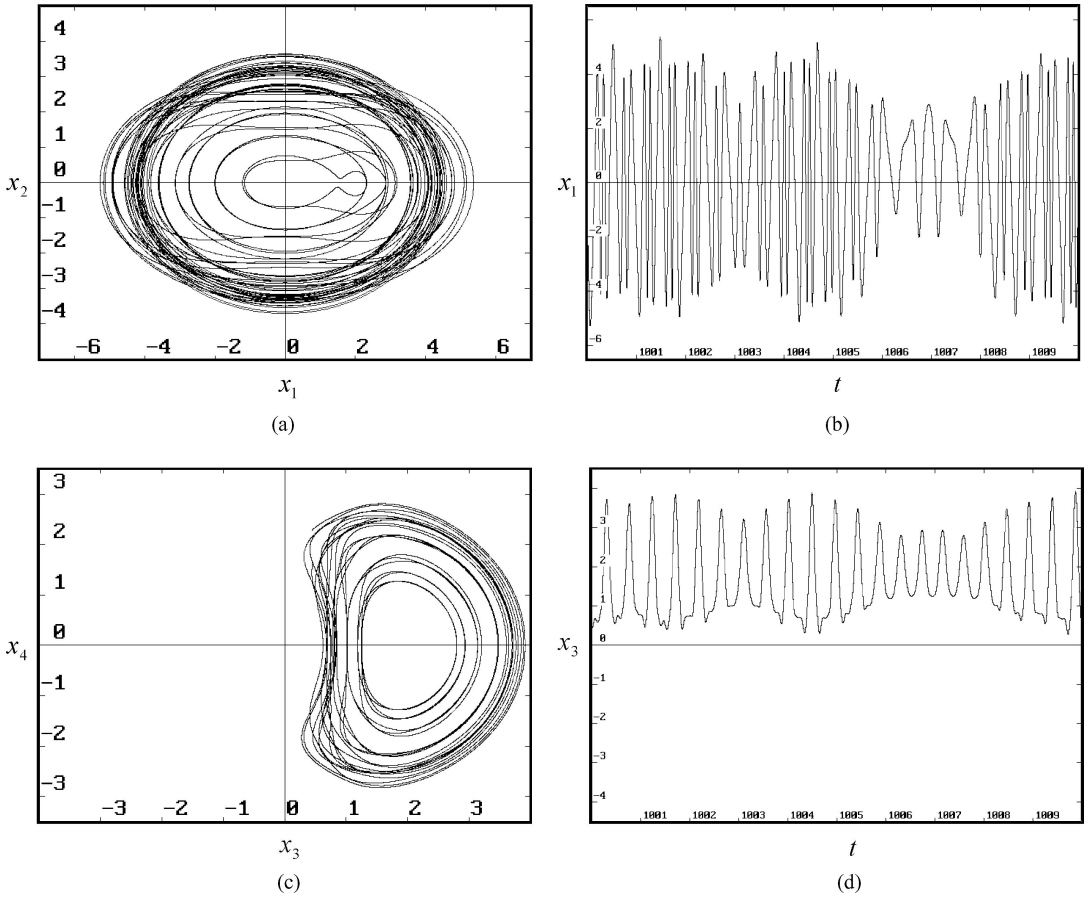

Figure 12. The chaotic responses in the nonlinear nonplanar oscillations of the cantilever beam for $F_1 = 11.7$, $f_2 = 36.8$, $c = 0.011$, $\sigma_1 = 2.0$, $\sigma_2 = 2.5$, $\alpha_1 = 1$, $\alpha_2 = -4.2$, $\alpha_3 = 2.01$, $\beta_1 = 3.1$, $\beta_2 = -0.43$, $x_{10} = 0.185$, $x_{20} = 0.655$, $x_{30} = 0.35$, $x_{40} = 0.18$; (a) the phase portrait on plane $(x_1,\ x_2)$; (b) the waveform on plane $(t,\ x_1)$; (c) phase portrait on plane $(x_3,\ x_4)$; (d) the waveform on plane $(t,\ x_3)$.

beam is shown in Figure 11. Other parameters including the transverse excitation in the z-direction and initial conditions in Figure 11 are the same as those in Figure 10. We find that the forms of the chaotic motions given by Figures 8 and 9 and Figures 10 and 11 are completely different.

When we respectively change the parametric excitation, transverse excitation in the z-direction, parameters and initial conditions to $F_1 = 11.7$, $f_2 = 36.8$, $c = 0.011$, $\sigma_1 = 2.0$, $\sigma_2 = 2.5$, $\alpha_1 = 1$, $\alpha_2 = -4.2$, $\alpha_3 = 2.01$, $\beta_1 = 3.1$, $\beta_2 = -0.43$, $x_{10} = 0.185$, $x_{20} = 0.655$, $x_{30} = 0.35$, $x_{40} = 0.18$, another form of chaotic response in the nonlinear nonplanar oscillations of the cantilever beam is shown in Figure 12. Figure 13 gives the chaotic response of the cantilever beam when the parameter β_2 changes to $\beta_2 = -3.83$. Other parameters including the parametric excitation, transverse excitation in the z-direction and initial conditions in Figure 13 are the same as those in Figure 12.

In Figure 14, the chaotic response of the cantilever beam is discovered when we choose the parametric excitation, transverse excitation in the z-direction, parameters and initial conditions as $F_1 = 61.7$, $f_2 = 86.8$, $c = 0.11$, $\sigma_1 = 2.0$, $\sigma_2 = 6.5$, $\alpha_1 = 1$, $\alpha_2 = -4.2$, $\alpha_3 = 2.01$, $\beta_1 = 5.1$, $\beta_2 = -0.23$, $x_{10} = 0.185$, $x_{20} = 0.655$, $x_{30} = 0.35$, $x_{40} = 0.18$.

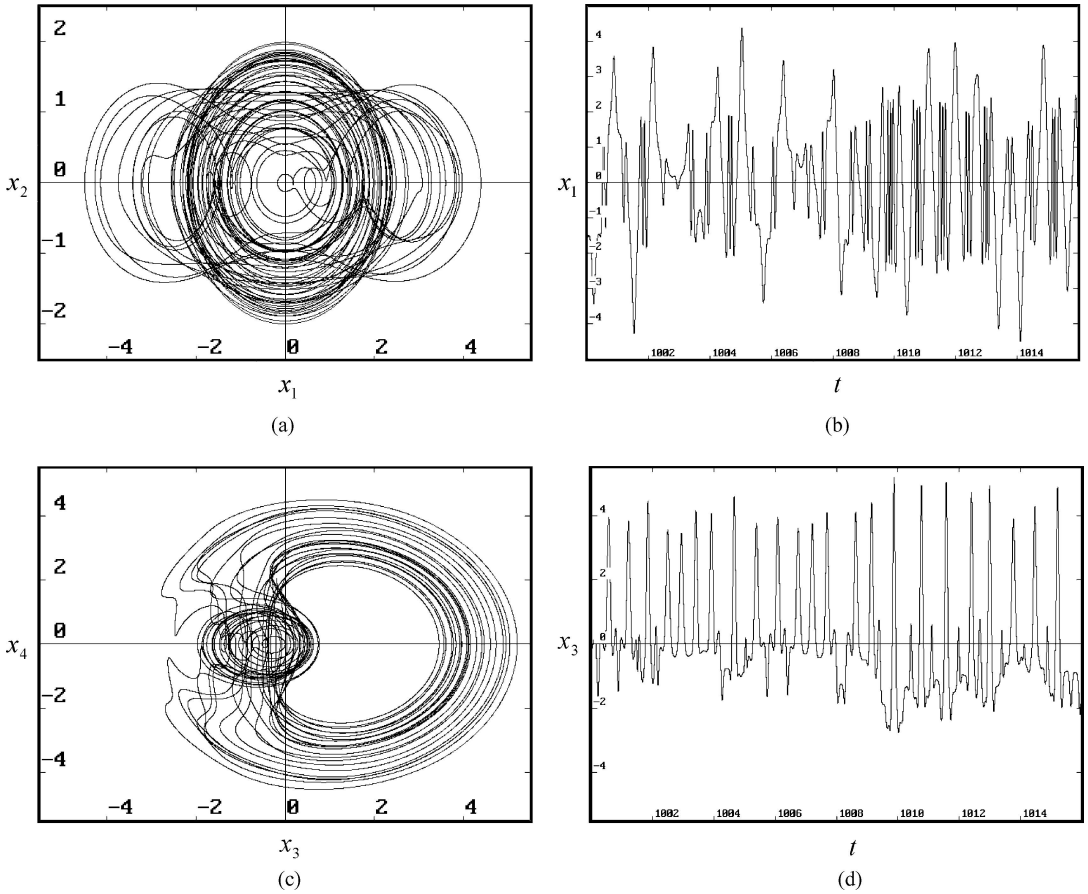

Figure 13. The chaotic responses in the nonlinear nonplanar oscillations of the cantilever beam for $F_1 = 11.7$, $f_2 = 36.8$, $c = 0.011$, $\sigma_1 = 2.0$, $\sigma_2 = 2.5$, $\alpha_1 = 1$, $\alpha_2 = -4.2$, $\alpha_3 = 2.01$, $\beta_1 = 3.1$, $\beta_2 = -3.83$, $x_{10} = 0.185$, $x_{20} = 0.655$, $x_{30} = 0.35$, $x_{40} = 0.18$; (a) the phase portrait on plane $(x_1,\ x_2)$; (b) the waveform on plane $(t,\ x_1)$; (c) phase portrait on plane $(x_3,\ x_4)$; (d) the waveform on plane $(t,\ x_3)$.

8. Conclusions

The global bifurcations and chaotic dynamics in the nonlinear nonplanar oscillations of the cantilever beam subjected to a harmonic axial excitation and transverse excitations at the free end are investigated for the first time by using the analytical and numerical approaches when the averaged equations have one non-semisimple double zero and a pair of pure imaginary eigenvalues. The study is focused on co-existence of 2:1 internal resonance, principal parametric resonance-1/2 subharmonic resonance for the in-plane mode and fundamental parametric resonance–primary resonance for the out-of-plane mode in Equation (11). It is found from the aforementioned analytical investigation that the cantilever beam subjected to a harmonic axial excitation and transverse excitations at the free end can undergo the pitchfork bifurcation, Hopf bifurcation, heteroclinic bifurcations and the Silnikov type single-pulse homoclinic orbit to the saddle focus, which means that there exists the chaotic motion in full four-dimensional averaged system. In order to illustrate the theoretical predictions, the *Dynamics* software is used to perform numerical simulation. The numerical results also show the existence of chaotic motion in the averaged equations. It is well known that the chaotic motions in the averaged equations can

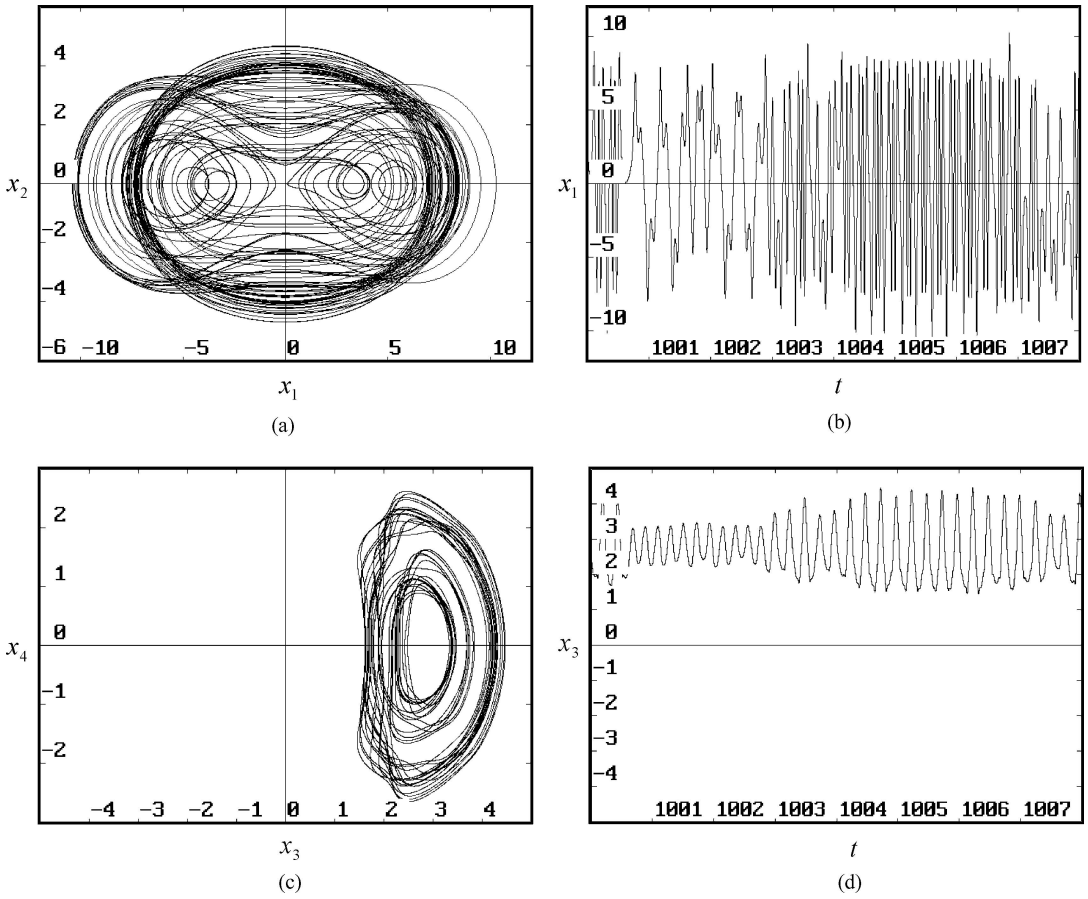

Figure 14. The chaotic responses in the nonlinear nonplanar oscillations of the cantilever beam for $F_1 = 61.7$, $f_2 = 86.8$, $c = 0.11$, $\sigma_1 = 2.0$, $\sigma_2 = 6.5$, $\alpha_1 = 1$, $\alpha_2 = -4.2$, $\alpha_3 = 2.01$, $\beta_1 = 5.1$, $\beta_2 = -0.23$, $x_{10} = 0.185$, $x_{20} = 0.655$, $x_{30} = 0.35$, $x_{40} = 0.18$; (a) the phase portrait on plane $(x_1,\ x_2)$; (b) the waveform on plane $(t,\ x_1)$; (c) phase portrait on plane $(x_3,\ x_4)$; (d) the waveform on plane $(t,\ x_3)$.

lead to the amplitude modulated chaotic oscillations in the original system under certain conditions. Therefore, it is demonstrated that there are the amplitude modulated chaotic motions of the Silnikov type in the cantilever beam subjected to a harmonic axial excitation and transverse excitations at the free end.

Numerical simulations obtained in this paper indicate that there exist different forms of the chaotic responses in the nonlinear nonplanar oscillations of the cantilever beam under certain parametric excitation, transverse excitation in the z-direction, parameters and initial conditions. It is found from numerical simulations that the shape of the chaotic motions in the in-plane mode is completely different from that in the out-of-plane mode. We also find that the parametric excitation F_1, transverse excitation in the z-direction f_2, damping coefficient c and parameter β_2 have important influence on the chaotic motions in the nonlinear nonplanar oscillations of the cantilever beam subjected to a harmonic axial excitation and transverse excitations at the free end. Moreover, the aforementioned analysis also illustrate that the in-plane and out-of-plane nonlinear oscillations of the cantilever beam must be simultaneously considered when the in-plane and out-of-plane principal flexural stiffnesses are different, that is, $\beta_y = D_\varsigma / D_\eta \neq 1$.

Acknowledgements

The authors gratefully acknowledge the support of the National Natural Science Foundation of China (NNSFC) through Grant Nos. 10372008 and 10328204, the National Science Foundation for Distinguished Young Scholars of China (NSFDYSC) through Grant No. 10425209, and the Natural Science Foundation of Beijing (NSFB) through Grant No. 3032006.

References

1. Crespo da Silva, M. R. M. and Glynn, C. C., 'Nonlinear flexural–flexural torsional dynamics of inextensional beams. I. Equation of motion', *Journal of Structural Mechanics* **6**, 1978, 437–448.
2. Crespo da Silva, M. R. M. and Glynn, C. C., 'Nonlinear flexural–flexural torsional dynamics of inextensional beams. II. Forced motions', *Journal of Structural Mechanics* **6**, 1978, 449–461.
3. Crespo da Silva, M. R. M. and Glynn, C. C., 'Out-of-plane vibrations of a beam including nonlinear inertia and nonlinear curvature effects', *International Journal of Non-Linear Mechanics* **13**, 1979, 261–271.
4. Crespo da Silva, M. R. M. and Glynn, C. C., 'Nonlinear nonplanar resonant oscillations in fixed-free beams with support asymmetry', *International Journal of Solids and Structures* **15**, 1979, 209–219.
5. Zaretzky, C. L. and Crespo da Silva, M. R. M., 'Experimental investigation of non-linear modal coupling in the response of cantilever beams', *Journal of Sound and Vibration* **174**, 1994, 145–167.
6. Nayfeh, A. H. and Pai, P. F., 'Non-linear non-planar parametric responses of an inextensional beam', *International Journal of Non-Linear Mechanics* **24**, 1989, 139–158.
7. Pai, P. F. and Nayfeh, A. H., 'Non-linear non-planar oscillations of a cantilever beam under lateral base excitations', *International Journal of Non-Linear Mechanics* **24**, 1990, 455–474.
8. Cusumano, J. P. and Moon, F. C., 'Chaotic non-planar vibrations of the thin elastica. Part I. Experimental observation of planar instability', *Journal of Sound and Vibration* **179**, 1995, 185–208.
9. Cusumano, J. P. and Moon, F. C., 'Chaotic non-planar vibrations of the thin elastica. Part II. Derivation and analysis of a low-dimensional model', *Journal of Sound and Vibration* **179**, 1995, 209–226.
10. Anderson, T. J., Nayfeh, A. H., and Balachandran, B., 'Coupling between high-frequency modes and a low-frequency mode: Theory and experiment', *Nonlinear Dynamics* **11**, 1996, 17–36.
11. Arafat, H. N., Nayfeh, A. H., and Chin, C. M., 'Nonlinear nonplanar dynamics of parametrically excited cantilever beams', *Nonlinear Dynamics* **15**, 1998, 31–61.
12. Esmailzadeh, E. and Nakhaie-Jazar, G., 'Periodic behavior of a cantilever beam with end mass subjected to harmonic base excitation', *International Journal of Non-Linear Mechanics* **33**, 1998, 567–577.
13. Hamdan, M. N., Al-Qaisia, A. A., and Al-Bedoor, B. O., 'Comparison of analytical techniques for nonlinear vibrations of a parametrically excited cantilever', *International Journal of Mechanical Sciences* **43**, 2001, 1521–1542.
14. Siddiqui, S. A. Q., Golnaraghi, M. F., and Heppler, G. R., 'Large free vibrations of a beam carrying a moving mass', *International Journal of Non-Linear Mechanics* **38**, 2003, 1481–1493.
15. Malatkar, P. and Nayfeh, A. H., 'On the transfer of energy between widely spaced modes in structures', *Nonlinear Dynamics* **31**, 2003, 225–242.
16. Young, T. H. and Juan, C. S., 'Dynamic stability and response of fluttered beams subjected to random follower forces', *International Journal of Non-Linear Mechanics* **38**, 2003, 889–901.
17. Wiggins, S., *Global Bifurcations and Chaos-Analytical Methods*, Springer-Verlag, New York, Berlin, 1988.
18. Kovacic, G. and Wiggins, S., 'Orbits homoclinic to resonance with an application to chaos in a model of the forced and damped sine-Gordon equation', *Physica D* **57**, 1992, 185–225.
19. Kovacic, G. and Wettergren, T. A., 'Homoclinic orbits in the dynamics of resonantly driven coupled pendula', *Zeitschrift für Angewandte Mathematik und Physik* (ZAMP) **47**, 1996, 221–264.
20. Kaper, T. J. and Kovacic, G., 'Multi-bump orbits homoclinic to resonance bands', *Transactions of the American Mathematical Society* **348**, 1996, 3835–3887.
21. Camassa, R., Kovacic, G., and Tin, S. K., 'A Melnikov method for homoclinic orbits with many pulse', *Archive for Rational Mechanics and Analysis* **143**, 1998, 105–193.
22. Haller, G. and Wiggins, S., 'Orbits homoclinic to resonance: The Hamiltonian', *Physica D* **66**, 1993, 298–346.
23. Haller, G. and Wiggins, S., 'Multi-pulse jumping orbits and homoclinic trees in a modal truncation of the damped-forced nonlinear Schrodinger equation', *Physica D* **85**, 1995, 311–347.
24. Haller, G. and Wiggins, S., '*N*-pulse homoclinic orbits in perturbations of resonant Hamiltonian systems', *Archive for Rational Mechanics and Analysis* **130**, 1995, 25–101.

25. Haller, G., *Chaos Near Resonance*, Springer-Verlag, New York, Berlin, 1999.
26. Feng, Z. C. and Wiggins, S., 'On the existence of chaos in a parametrically forced mechanical systems with broken O(2) symmetry', *Zeitschrift für Angewandte Mathematik und Physik* (ZAMP) **44**, 1993, 201–248.
27. Feng, Z. C. and Sethna, P. R., 'Global bifurcations in the motion of parametrically excited thin plate', *Nonlinear Dynamics* **4**, 1993, 389–408.
28. Feng, Z. C. and Liew, K. M., 'Global bifurcations in parametrically excited systems with zero-to-one internal resonance', *Nonlinear Dynamics* **21**, 2000, 249–263.
29. Malhotra, N. and Sri Namachchivaya, N., 'Global dynamics of parametrically excited nonlinear reversible systems with nonsemisimple 1:1 internal resonance', *Physica D* **89**, 1995, 43–70.
30. Malhotra, N. and Sri Namachchivaya, N., 'Chaotic dynamics of shallow arch structures under 1:1 internal resonance', *ASCE Journal of Engineering Mechanics* **123**, 1997, 620–627.
31. Malhotra, N., Sri Namachchivaya, N., and McDonald, R. J., 'Multipulse orbits in the motion of flexible spinning discs', *Journal of Nonlinear Science* **12**, 2002, 1–26.
32. Yagasaki, K., 'Periodic and homoclinic motions in forced, coupled oscillators', *Nonlinear Dynamics* **20**, 1999, 319–359.
33. Zhang, W., Liu, Z. M., and Yu, P., 'Global dynamics of a parametrically and externally excited thin plate', *Nonlinear Dynamics* **24**, 2001, 245–268.
34. Zhang, W., 'Global and chaotic dynamics for a parametrically excited thin plate', *Journal of Sound and Vibration* **239**, 2001, 1013–1036.
35. Zhang, W. and Li, J., 'Global analysis for a nonlinear vibration absorber with fast and slow modes', *International Journal of Bifurcation and Chaos* **11**, 2001, 2179–2194.
36. Zhang, W. and Tang, Y., 'Global dynamics of the cable under combined parametrical and external excitations', *International Journal of Non-Linear Mechanics* **37**, 2002, 505–526.
37. Wang, F. X., 'Nonlinear oscillations and global dynamics of flexible cantilever beams', *Master Thesis*, Beijing University of Technology, 2002.
38. Nayfeh, A. H. and Mook, D. T., *Nonlinear Oscillations*, Wiley-Interscience, New York, 1979.
39. Zhang, W., Wang, F. X., and Zu, J. W., 'Computation of normal forms for high dimensional nonlinear systems and application to nonplanar motions of a cantilever beam', *Journal of Sound and Vibration* **278**, 2004, 949–974.
40. Yu, P., Zhang, W., and Bi, Q. S., 'Vibration analysis on a thin plate with the aid of computation of normal forms', *International Journal of Non-Linear Mechanics* **36**, 2001, 597–627.
41. Nusse, H. E. and Yorke, J. A., *Dynamics: Numerical Explorations*, Springer-Verlag, New York, Berlin, 1997.